1971

Tests of composite beams under negative moment, February 1971

I. Garcia

J. Hartley Daniels

TESTS OF COMPOSITE BEAMS UNDER NEGATIVE MOMENT

by

I. Garcia

J. Hartley Daniels

This research was conducted by
Fritz Engineering Laboratory
Lehigh University
for
Pennsylvania Department of Transportation
in Cooperation with
U. S. Department of Transportation

Fritz Engineering Laboratory
Department of Civil Engineering
Lehigh University
Bethlehem, Pennsylvania

February 1971

Fritz Engineering Laboratory Report No. 359.1

ABSTRACT

Five composite steel-concrete beams were tested under negative bending moment (slab in tension). The purpose of the tests was as follows:

(1) To investigate the effect of the amount of longitudinal reinforcing steel in the slab, and

(2) To determine whether or not it is possible to simulate the negative moment region of a continuous composite beam by using a simple span beam subjected to negative bending moment.

Although five composite beams were tested only four are described in detail in this report. The four composite beams reported herein were given the following designations: CC-3F, CC-4F, SC-3S and SC-4S.

All of the beams consisted of a reinforced concrete slab 60 inches wide and 6 inches thick, connected to a W21x62 rolled steel beam by 3/4 in. x 4 in. stud shear connectors. CC-3F and CC-4F were 50'-10" long continuous composite beams with two equal spans of 25'-0. SC-3S and SC-4S were 15'-4" long. Simple span composite beams which were designed to simulate the negative moment region of the continuous composite beams mentioned above. CC-3F and SC-3S had a longitudinal reinforcement percentage of 0.61% while CC-4F and SC-4S had a longitudinal reinforcement

percentage of 1.02%. All four beams were loaded to ultimate, however, CC-3F and CC-4F were first subjected to over 2 million cycles of working load.

Based on the tests described in this report, the following was concluded:

(1) The tensile capacity of the longitudinal steel reinforcement of the slab should be larger than the tensile capacity of the concrete alone.

(2) Simple span beams loaded under negative moment conditions can be used to study the negative moment region of continuous composite beams.

(3) An accurate theory is required to predict the stresses in continuous composite beams in which there are no shear connectors over a substantial length of the negative moment region.

TABLE OF CONTENTS

1. INTRODUCTION

Simple span composite bridges are quite common in most states, but the relatively small number of continuous composite bridges constructed reflects a lack of confidence in the ability to produce satisfactory structures of this type. A need therefore exists for more detailed design specifications and a specific method of analysis for this type of structure. There is also the need for the development of design criteria which will provide for satisfactory control of cracking in the concrete slab and specification provisions to guard against fatigue failure of certain elements of the cross-section subjected to negative moment.

The basic design criteria and procedures for proportioning shear connectors in steel-concrete composite bridge members have been developed for simple spans in recent studies at Lehigh University.[1]* These studies suggest that the above design criteria are also applicable to continuous beams.

Continuous composite beams designed by the AASHO specifications may be composite or non-composite in the negative moment region.[2] It appears that in practice the majority of continuous composite bridges are designed without shear connectors in

---

* References are listed at the end of this report.

the negative moment region. In this case, the AASHO specifications state that additional anchorage connectors shall be placed in the region of the point of dead load contraflexure. The number of additional connectors required is a function of (1) the total area of the longitudinal slab reinforcement that is continuous through the negative moment region, (2) the range of stress in the reinforcement due to live load plus impact (or 10,000 psi in lieu of more accurate computations) and (3) the allowable range of horizontal shear on an individual shear connector (fatigue requirement).

The AASHO Specifications also state that the additional anchorage connectors shall be placed adjacent to the point of dead load contraflexure within a distance equal to 1/3 the effective slab width and placed either side of this point or centered about it.

The above mentioned pilot studies confirmed the recommendations suggested in Ref. 3. It was shown clearly that shear connectors are required to resist the force developed in the continuous longitudinal reinforcing steel in negative moment regions. These studies showed that a force is developed in the reinforcing steel even though shear connectors are omitted and the reinforcement is neglected when proportioning the cross-section for negative moment. It is apparent that most of this force arises

due to anchorage of the longitudinal reinforcing steel in the positive moment regions. Additional force is developed because the slab in the negative moment region must conform approximately to the curvature of the steel beam. The pilot study confirmed that the effect of the tension forces being applied to the slab is to cause cracking in the slab throughout the negative moment region and overstressing of shear connectors in the adjacent positive moment regions due to the high anchorage forces. To reduce the shear connector stresses, additional anchorage connectors are therefore required in order to transfer the tension force in the longitudinal reinforcement to the steel beam.

The pilot studies also revealed that additional study of all of the various factors involved in the design of the negative moment region was needed. As a result, current investigations are concentrating on such factors as (1) the extent to which connectors can be omitted in the negative moment region, (2) the optimum requirements for longitudinal reinforcement in the negative moment region with respect to fatigue behavior and slab cracking, and (3) the stress conditions that exist in continuous composite beams during the passage of vehicles.[4,7,8]

Initially, experimental and theoretical studies were carried out using two, two-span continuous composite test beams of the same spans and geometry as those previously reported in

Ref. 1. The results of these studies are reported in Ref. 4. It was considered desirable to further study the significant variables which affect the behavior of continuous composite beams in the negative moment region by using shorter simple span beams intended to simulate the negative moment region of the test beams reported in Ref. 4. As the first step in this parallel study, three simple span composite pilot beams were designed and tested under negative bending moment (slab in tension) to verify if the indicated variables could be effectively studied in this manner.

The first two simple span test beams (each designated SC-3S) were made identical but were tested in two different ways in order to determine which test set-up should be used for SC-4S and for future tests. Only the results from one of these test beams is reported herein, and in this report that beam is designated CC-3S. Figure 10 shows schematically the test set-up found to be satisfactory. The unsatisfactory test set-up was a simplification of that shown in Fig. 10 in which the composite beam with the slab on the bottom (instead of on top as shown in the figure) was simply supported at the two ends and loaded at the center to produce a slab in tension condition. The results were questionable because the slab separated from the steel beam and sagged between the connected regions.

It was found that the essential behavior of the negative

moment region of continuous composite beams could be studied using simple span beams and the test set-up in Fig. 10. The information obtained from these pilot tests was used to design four additional test beams, the results of which will be the subject of a subsequent report.[7]

Details of the design, fabrication, instrumentation, and testing of beams SC-3S and SC-4S and the analysis of the test results are presented fully in this report. For beams CC-3F and CC-4F many of the above details are presented in Ref. 4. However, additional information regarding beams CC-3F and CC-4F is presented in this report where that information directly relates to the objective of the study reported herein.

2. TEST BEAMS, INSTRUMENTATION AND TESTING PROCEDURE

2.1 Description of Test Beams

Figure 1 shows the two types of composite beams that were tested in this investigation. The test beams designated CC-3F and CC-4F (Fig. 1a) were each two-span continuous composite beams. They were 50'-10" long overall with two equal spans of 25'-0. These beams consisted of a reinforced concrete slab 60 inches wide and 6 inches thick, connected to a W21X62 rolled steel beam by 3/4 in. x 4 in. stud shear connectors. Further details of these two beams are reported in Ref. 4.

The test beams designated SC-3S and SC-4S (Fig. 1b) were each simple span composite beams 15'-4" long overall. These beams were identical to the 12'-8" region between the dead load points of contraflexure of the continuous beams CC-3F and CC-4F respectively. They also included a 16-inch projection into the positive moment region each side as shown in Fig. 1b. A typical cross-section for all four beams is shown in Fig. 1c.

2.2 Design Criteria

The design criteria for beams SC-3S and SC-4S were the same as for the continuous composite beams CC-3F and CC-4F. The

design criteria for beams CC-3F and CC-4F are reported in Ref. 4 and further discussed in Ref. 1.

2.3 Design Details and Fabrication

Fabrication details for beams CC-3F and CC-4F are reported in Ref. 4.

Fabrication details for beams SC-3S and SC-4S are shown in Fig. 2. The rolled steel beams were of ASTM A36 steel. They were cut from 55-ft. rolled shapes by a local fabricator. Bearing stiffeners and stud shear connectors (Fig. 2a) were welded by the fabricator. Unused sections of the rolled shapes were sent to Fritz Laboratory to provide material for tension tests of the steel beam as well as for the welded studs.

Before welding the shear connectors to the rolled steel beams, the equipment was adjusted following tests of several studs which were welded to the excess lengths of the beams. The quality of the welds was verified using the inspection procedure outlined in Ref. 2.

Figure 2b shows the stud shear connector patterns used as determined from the design conditions. Fig. 2c shows a typical cross-section of the fabricated steel beam with connectors, stiffeners and loading pins. The loading pins were located approximately

at the center of gravity of the composite section under negative bending moment (slab in tension). These pins were welded to the end bearing stiffeners which were welded to the rolled steel beams.

2.4 Construction

Construction details of beams CC-3F and CC-4F are reported in Ref. 4.

Figure 3 shows the slab formwork for one of the short test beams and the reinforcement and instrumentation in place ready for pouring the concrete slab. The forms were re-used for the other short test beam. Each beam was continuously supported from the laboratory floor during concrete pouring.

The concrete was proportioned and transit-mixed for a 28 day compressive strength of 3000 psi with a slump of 3-1/2 in. Consolidation was accomplished by internal vibration as placement progressed. The final finish was obtained by hand trowelling. Twelve control cylinders were poured for each concrete slab, six at the beginning and six at the end of each pour.

The concrete in the slabs was moist cured for seven days together with four cylinders. Moist curing was accomplished by covering the exposed surface with wet burlap and a polyethylene sheet. The forms were removed approximately 14 days after casting

and the slabs were allowed to cure under dry conditions until the beams were tested. Testing of each beam occurred between 60 and 90 days following pouring. Eight of the control cylinders from each beam were maintained as prescribed by ASTM for the standard f'_c test. The remaining four cylinders were cured along with the beam.

2.5 Properties of the Test Beams

A test program was conducted to determine the mechanical properties of the materials used in the test beams. Properties of the structural steel were determined from tensile coupons cut from the control pieces left over from the rolled shapes used for the test beams. Mechanical properties of the steel are shown in Table 1. The coupons were tested in a 120 kip Tinus Olsen Universal machine at a speed of 0.025 in per minute up to first yielding and then at 0.3 in per min. until fracture occurred. For all coupon tests the yield point, the static yield level, and the ultimate load were recorded. In addition a plot of applied tension versus elongation was obtained. The modulus of elasticity and the strain hardening modulus were not determined from the tension control lests. Where required, standard values are assumed (Ref. 5).

The mechanical properties of the No. 4 and No. 5 deformed reinforcing bars were determined by tension tests on 2 ft. lengths of bar. These results are also shown in Table 1.

The concrete used for the slabs was made of type 1 Portland cement, crushed gravel and natural bank sand. The slabs were poured one at a time and control cylinders taken as previously reported. The concrete cylinder test results are shown in Table 2.

The physical dimensions of the test beam components were measured and the cross section properties of the test beams were determined. The values obtained are shown in Tables 3 and 4. The measured values for the rolled shapes are also compared with AISC manual values in Table 3.

2.6 Instrumentation

The instrumentation for beams SC-3S and SC-4S was essentially the same. Figures 4 to 9 summarize the details of the instrumentation used for the test beams in this investigation. A combination of electrical resistance strain gages, dial gages and level bar rotation gages was used.

Figure 4 shows the location of the SR-4 electrical strain gages which were used to determine the flexural strains in the rolled steel beams and the slab reinforcement. A typical instrumented cross-section had eleven electrical strain gages placed on the longitudinal reinforcement bars, six more on the transverse reinforcement bars, and another ten in the rolled steel beam.

A schematic view of the protection used for the strain

gages on the longitudinal and transverse slab reinforcement is shown in Fig. 5. The strains were measured in a uniformly stressed bar section, free from the gripping action of the surrounding concrete.

A close up detail for the reinforcement bar strain gages as they appeared ready for pouring the concrete is shown in Fig. 6b.

Figure 6a shows additional instrumentation provided at each cross-section for measuring slab separation and slip. This consisted of two Ames 0.001-in. mechanical dial gages at each cross-section. One dial gage was positioned with the plunger in a horizontal position to measure the slip at the interface. The other one had the plunger positioned for vertical measurements and recorded the uplifting of the concrete slab from the rolled steel beam. Both gages were fixed to a vertical rod welded to the upper flange of the rolled beam and their plungers rested against a 14 gage steel plate bent into an L shape and bolted to the concrete.

Figures 7 and 8 show the instrumented cross-sections for the test beams. Fig. 7 corresponds to beams SC-3S and SC-4S. Beam SC-3S had 9 instrumented sections while beam SC-4S was instrumented only at sections 1 to 6. Fig. 8 corresponds to beams CC-3F and CC-4F (Ref. 1). These beams had only 3 instrumented sections in the negative moment region corresponding to instrumented sections

1, 3 and 5 of the simply supported test beams, SC-3S and SC-4S.

Level bar rotational gages as well as vertical deflection gages (Fig. 7) were also provided in order to obtain the end rotation and vertical deflections of the test beams.

The recording equipment consisted in two DATRAN units and one Budd strain indicator to read the electrical resistance strain gages, as well as one fifty power microscope to read the width of the cracks which developed in the concrete slab during the test.

2.7 Test Procedure and Loading

The loading procedure for beams SC-3S and SC-4S simulated the loading procedure for the continuous beams. The center of beams SC-3S and SC-4S was supported while vertical shear forces were applied at the points of contraflexure by loading directly into the web of the rolled steel beam as shown in Fig. 1b. These beams therefore behaved as double cantilevers having a 6'-4" span each side with an additional length of 16" to provide continuity and anchorage of the longitudinal reinforcement in the concrete slab.

In this report test results for all four beams are discussed mostly with reference to two load levels - a predicted

working load level of 60^k and a level of 150^k which was near the ultimate load level. For beams CC-3F and CC-4F allowable stresses are reached at a predicted center reaction of about 60^k(Fig. 1a).[4] This is designated the working load level for those beams. Similarly, near ultimate load occurred at center reaction of about 150^k. For beams SC-3S and SC-4S (which were designed to simulate the negative moment regions of beams CC-3F and CC-4F respectively) allowable stresses were predicted when the center reaction was approximately 60^k and near ultimate load was reached when the center reaction was about 150^k(Fig. 1b). The predicted load corresponding to first yielding in the four beams was approximately 100^k. The predicted and observed load-deflection behavior of the four beams is shown in Fig. 19.

Test beams SC-3S and SC-4S were first supported and loaded in such a way as to produce a positive bending moment in the beams(slab in compression). This was done in order to break the bond developed between the upper flange of the rolled beam and the concrete slab. The beams were supported at both ends by 6-in. diameter steel rollers. Longitudinal stability was maintained by the cross-head of the testing machine. The load was applied by the 5,000,000 lb. Baldwin testing machine located in Fritz Laboratory and was small enough to produce elastic response in the beams. A 4-ft. long beam distributed the load across the slab

width to a 4-in. wide homesote pad bearing against the concrete surface. Both beams were then tested under negative bending moments.

Figures 9 and 10 show the test setup used to test the beams under negative bending moment. The load was applied to one end of the test beam using the 5,000,000 lb. Baldwin Testing Machine in Fritz Laboratory and a lever bar mechanism which is shown schematically in Fig. 10. The lever bar was supported by a roller at one end, loaded by the testing machine at its center and connected to the test beam at the other through a tension hanger. The test beam was supported at its center by a 4 in. roller and at its other end by another tension hanger which was attached to the apron of the testing machine. The tension hangers were pin connected to the test beam and to the lever bar and the apron.

The tests were carried out approximately nine to ten weeks after pouring the concrete. Each test required approximately 12 hours to complete and was carried out on 2 consecutive days. Twenty kip load increments were applied up to first yielding. After first yielding ten kip load increments or less were applied until the ultimate load was reached. After each load increment the load was held constant until deformations had ceased. The data was then recorded and the next load increment applied. As

plastic deformations began to take place, the period of time for the stabilization of deformations increased up to 30 min. In the vicinity of the ultimate load deflection increments were used instead of load increments, enabling the unloading behavior of the beams to be obtained.

3. TEST RESULTS AND ANALYSIS

3.1 Strain Distribution

3.1.1 Longitudinal Reinforcement

Figure 11 shows the average strain distribution in the londitudinal slab reinforcement for test beams SC-3S and SC-4S, at two load levels. Also shown for comparison is the average strain distribution in the longitudinal slab reinforcement for the same load levels for the two span continuous beams CC-3F and CC-4F. Two load levels were selected to illustrate typical test results. The first is the working load level as determined by the allowable stresses and corresponds to approximately 60 kips vertical reaction at the center support.[4] The second is a load level near the ultimate load which corresponds to about 150 kips vertical reaction at the center support. The average of the measured strains for beams SC-3S and SC-4S for the 60^{k} and 150^{k} load levels are indicated by the solid circles and squares respectively. The open circles and open squares indicate the average of the strains for the two continuous beams CC-3F and CC-4F. The dashed lines represent the theoretical values as computed from simple tie bar theory assuming that only the steel section (rolled steel beam plus reinforcing bars having fully developed anchorage) is effective in the negative moment region. The strains in the longitudinal reinforcing for beam CC-3F at the 150 kip load level are not

shown because of a fatigue failure of some of the longitudinal reinforcing bars which occurred during the fatigue test as reported in Ref. 4.

It can be observed from Fig. 11 that a considerable variation in strain distribution occurred between beams SC-3S and SC-4S. In beam SC-3S the strain distribution was very irregular. It was observed for this beam that peaks of strain were located in the vicinity of cracks in the concrete slab (crack locations are not shown in the figure). Minimum strain values were observed to occur between the cracks. In addition, large strains were measured in SC-3S even at the working load level.

The distribution of strains for test beam SC-4S exhibited more predictable behavior and smaller strains were recorded. Although it was again observed that the largest strains occurred in the vicinity of cracks, there was a larger number of cracks in beam SC-4S and a more uniform crack spacing.

The test results illustrated in Fig. 11 indicated that a closer and more uniform crack pattern in the slab resulted from a larger amount of longitudinal slab reinforcement. Also, a more predictable distribution of longitudinal reinforcement strains was achieved.

It can also be observed from Fig. 11a that a correlation

in the strains for beams SC-3S and CC-3F did not occur at corresponding sections. Nevertheless, the level of maximum strains in the unconnected regions in the two beams was in fairly good agreement. Much better correlation in the strains of beams SC-4S and CC-4F was obtained as shown in Fig. 11b.

The results presented in Fig. 11 indicate that in all cases the theoretical strains computed from simple tie bar theory were smaller than the maximum strains measured.

In the theoretical predictions no modification of reinforcement area due to shear lag and transverse slab deformations was considered. The observed difference between the test results and the theoretical predictions was largest in beams SC-3S and CC-3F which had the least reinforcement. In this case theory predicts about 50% of the maximum average measured strains. In beams SC-4S and CC-4F where the amount of slab reinforcement was greater, the predicted values are closer to the measured values but are still unconservative and about 11% smaller on the average.

Figures 12 and 13 show the strain distributions at the mid-depth of the slab for all four beams. The strains were determined by averaging the measured strains in the upper and lower longitudinal reinforcing bars. As before, two load levels are considered - a working load of 60 kips and a yield load of 150 kips

(Refer to Art. 2.7). Fig. 12 compares the results for beams SC-3S and CC-3F. Fig. 13 compares the results for beams SC-4S and CC-4F. Two characteristic types of strain distribution can be seen. One corresponds to a fairly low strain level and shows a relatively uniform strain distribution across the slab. This is typical for a cross-section between cracks. The other shows a fairly high strain level and has an irregular distribution. This is characteristic of a cross-section at a crack or in its immediate vicinity.

For beams SC-3S and CC-3F which have the smaller amount of longitudinal slab reinforcement the strains at the cross-sections appear either very small or very large depending upon the crack locations. The strain distribution for SC-3S at 150 kips is not shown at Section 5 because it is beyond the scale of the figure.

Similarities in the level and distribution of strains can be seen to occur between corresponding test beams (simple span versus continuous). As previously discussed, this situation occurs whenever the same cracking conditions of the slab are present at corresponding sections. Local differences in strains are due to several factors such as bond between the concrete and the wires leading to the individual strain gages and torsional moments in the beams due to irregularities in construction and loading.

A more detailed strain distribution at Section 3 of test beams SC-4S and SC-4F is shown in Fig. 14. This figure shows the difference between the measured strains in the upper and lower layers of the longitudinal reinforcement bars. The upper layer strain values are less than the strain values for the lower layers. This is a typical result obtained at all load levels for all four beams, at both Sections 2 and 3. These two sections are nearest the shear connectors as shown in Fig. 11. Simple tie-bar theory does not explain this situation. This theory also does not include the general tendency of the strains in the bars over the steel beam to rise over the strains further out in the slab.

It can be concluded from observations of the longitudinal strains in the four test beams that in general the strains in beams SC-3S and SC-4S did correlate fairly well with similar strains in beams CC-3F and CC-4F but that simple tie-bar theory is inadequate for accurately predicting these strains.

3.1.2 Transverse Reinforcement Strains

In Fig. 15 the transverse reinforcement strains at several cross-sections of beam SC-4S are compared. These results are typical for all load levels. A complex distribution of the transverse strains is indicated. Sign reversals for strains in the same bar were frequent as were fluctuations of strains between

the several cross-sections. The strain distributions for the other three test beams showed a similar behavior. It was observed from the test data that the transverse reinforcement strains were produced by a combination of flexural strains in two perpendicular directions - one in the plane of the slab in the direction of the longitudinal axis, and the other perpendicular to the plane of the slab. Torsional strains also contributed to the observed variation. No specific trends were apparent for the four beams; nevertheless, the influence of the crack locations and the boundary conditions in the neighborhood of the contraflexure region for the continuous beams or the end of the beams for the simply supported beams can be observed.

Corresponding beams SC-4S and CC-4F presented some similarities in transverse strain distribution. The signs of the strains were the same, and the orders of magnitude (small in all cases) also agreed. Corresponding beams SC-3S and CC-3F did not present this similarity in behavior.

3.2 Bending Moment Distribution

Figures 16 and 17 show the distribution of negative bending moments for the four beams at the 60^{k} and 150^{k} load levels. The solid line is the moment distribution found from equilibrium conditions using the measured vertical reaction at the center

support. The solid circles show the calculated values of the moments at each cross-section using the strain readings obtained at the cross-sections. The dashed line represents the predicted bending moments. For the simple span beams the predicted curve and the curve computed from equilibrium conditions based on the measured center reaction are the same. Tie-bar theory was used to predict the bending moments for the continuous beams. The bending moments at the 150 kip load level are not available for beam CC-3F (Fig. 16a) due to the reinforcement bar failure during fatigue as discussed previously.[4]

Good correlation is apparent between the moments calculated from the strain distribution at the cross-sections and the moments found from equilibrium using the measured center reaction. Although small variations are observed there is in general an overestimation of the moments corresponding to the 150 kip load level. This is probably due to the straining of the electrical wires leading to the strain gages which were embedded in the concrete. From the good agreement obtained between the bending moments computed from the measured strains and from the center reaction it can be concluded that due to the protection provided to the gages on the reinforcement bars accurate strains were measured. These results, however, could be further improved by shortening the length of the lead wire that is embedded in the

concrete and by protecting the lead wire inside the concrete to prevent bonding to the concrete. These and other improvements were made in four subsequent beam tests with somewhat better results.[7]

Figures 16 and 17 show the close correspondence of the moment diagrams obtained from the respective beams SC-3S and CC-3F, and SC-4S and CC-4F. Of particular interest is the location of the points of zero moment which were fixed (loading points) for the simple span beams. In each case the point of zero moment was located within a few inches (4-in. at the most) of the point of inflection for the continuous beams. As a result, the negative moment region was simulated to within 5% for beam CC-3F and 2% for beam CC-4F.

Figure 18 shows the distribution of horizontal forces in the concrete slabs at three load levels for beams SC-3S and SC-4S. The solid points represent the slab forces computed using the measured strains at the cross-sections. The open circles represent the forces computed from the corresponding strains in the continuous beams CC-3F and CC-4F. The dashed lines are the theoretical forces predicted using simple tie-bar theory where the slab in the region without connectors is assumed to be fully cracked. The load levels shown in the figure correspond to the two previously mentioned levels of 60 and 150 kips, plus an initial

yielding load level equivalent to approximately 100 kips measured at the vertical reaction of the center support of beams SC-3S and SC-4S and an applied load of approximately 100 kips for beams CC-3F and CC-4F.

It can be observed from Fig. 18 that within the region containing no shear connectors, the slab force (force in the longitudinal reinforcement) is fairly constant as assumed by simple tie-bar theory. The observed variations for the forces obtained from the measured strains are mainly due to variations in the cross-sectional properties at the instrumented cross-sections.

It is observed in Fig. 18a that at the 60 kip load the force in the slab of beam SC-3S is within the expected range. However, at the 100 kip load an abrupt change in force took place in the slab. The measured slab force was substantially greater than the predicted one. The increase in the slab force was much smaller as the load level was increased from 100 kips to 150 kips. The increase in slab force in beam SC-4S was much more uniform and followed the predicted increases more closely (Fig. 18b).

The observed difference in behavior between beams SC-3S and SC-4S in the vicinity of the initial yield load was probably due to the fact that the initial yield load as observed during test and the initial yield load as predicted by simple tie-bar

theory was somewhat closer for beam SC-4S than for beam SC-3S. This result again illustrates the inability of simple tie-bar theory to accurately predict the stresses in the longitudinal slab reinforcement for the beams considered in this investigation.

The above difference in behavior is important for the case of cyclic loading since the stress range in the reinforcement bars is an important parameter in the case of fatigue.

A comparison of the slab forces between the corresponding continuous and simple span beams at sections 1, 3, and 5 indicate that the average of the computed slab forces for corresponding beams agree to within 10% in the regions without shear connectors. The slab forces at Section 1 were slightly different because the boundary conditions were not the same. At Sections 3 and 5 fairly good correlation can be observed.

3.3 Load Deflection Behavior

Figure 19 shows the load deflection behavior of the four test beams. Load deflection curves for SC-3S and CC-3F are shown in Fig. 19a. Load deflection curves for beams SC-4S and CC-4F are shown in Fig. 19b. In each case the relative deflection between the center support and the inflection points is plotted.

It can be observed from the figures that all four beams

attained an ultimate load capacity that was within 2% of the ultimate load based on ultimate strength theory.[6] Except for beam SC-4S, a horizontal plateau was attained before unloading took place which occurred after the occurrence of local buckling in the compression flange as will be discussed later in this chapter.

The test results for the two continuous beams CC-3F and CC-4F were obtained after about 2,000,000 cycles of 0 to 60 kip loading had been applied.[4] The curve corresponding to 10 cycles of 0 to 60 kip loading is not shown in the figure but it overlaps the predicted curve up to the 60 kip level. The difference between the 10 cycle curve and the 2,000,000 cycle curve in the case of beam SC-3F is due to the fact that the upper layer of reinforcement in the slab of beam SC-3F had failed in fatigue by the time the ultimate strength test took place. As a result beam CC-3F was somewhat more flexible. For beam CC-4F the predicted and test curves corresponding to 10 and 2,000,000 cycles are nearly identical.

It is of interest to note the differences in initial yield loads for the corresponding beams SC-4S and CC-4F. It is also of interest to consider why the load deflection curve for beam CC-4F was steeper than the curve for beam SC-4S during the initial loading whereas the reverse was true at the higher load levels. These two phenomena can probably be explained as follows.

The cross-sectional properties for beam CC-4F were slightly different than the properties of beam SC-4S.(Ref. 4 and Table 3) Also the compatibility restrictions imposed at the point of contraflexure by the more rigid positive moment portion of the beam CC-4F and the more favorable cross-section properties of beam CC-4F tended to make beam CC-4F more stiff than beam SC-4S during initial loading.

At the time the ultimate strength test was conducted for beam CC-4F, the concrete slab of beam CC-4F was more heavily cracked than in beam SC-4S. This had the effect of altering the occurrence of initial yielding in the two beams. As a result yielding took place first in beam CC-4F. Beam SC-4S continued to exhibit greater stiffness than CC-4F until yielding also occurred in that beam. This developed when the crack pattern in beam SC-4S was about the same as that in beam CC-4F.

In general, however, the load deflection curves for corresponding beams indicated that a simulation of the continuous beam behavior was achieved with the simple span beams.

3.4 Force on the Shear Connectors

Table 5 summarizes the forces on the shear connectors for the four test beams. The forces acting on the shear connectors of the two continuous beams is shown corresponding to three stages of 0 to 60 kip fatigue loading as well as at the 100 and 150 kip

load levels after the 2,000,000 cycles of fatigue loading had been applied. The measured forces in the connectors of the simple span beams are shown for three load levels corresponding to 60, 100 and 150 kips at the center reaction. The total force to be resisted by the shear connectors is the force in the slab. The force in the slab was taken as the maximum force measured between Sections 3 and 5 since it was reasonably constant in this region and was not greatly affected by the friction force over the center support. The force per connector was estimated by dividing the slab force by the number of connectors included between Section 3 and the point where the force in the slab decreased to zero. Theoretical values for the average force per shear connector based on tie-bar theory are also provided, where the same number of connectors used to obtain the experimental values for the average force acting on the connectors, was considered to obtain the average theoretical force per connector.

It can be seen from Table 5 that the connectors for beam SC-3S experienced a large force increment as the load increased from 60 to 100 kips. It can also be seen that only a small increment of force was experienced by the connectors as the load increased from 100 to 150 kips. On the other hand the force increments in the connectors of beam SC-4S were small as the load increased from 60 to 150 kips.

It can also be observed that the shear force per connector for beam SC-3S at the 60 kip load level is less than the force per connector for beam CC-3F at the same load level at 10 cycles and at 600,000 cycles. This appears to be due to a lack of accuracy in measuring the force for beam SC-3S which was expected to exhibit a greater force in the slab. Beam SC-4S exhibited larger values than those obtained in beam CC-4F. It is logical that a greater slab force would develop in beam SC-4S because its slab was not as severely cracked as was the slab in beam CC-4F.

It can further be observed that the predicted values of connector forces are less than the experimental ones except for beam CC-3F at the 150 kip load level where the reinforcement bars had reached their yield capacity.

3.5 Slip and Slab Separation

Figures 20 to 22 show the magnitude of the slip and slab separation obtained in the four test beams between the steel beam and slab. The measured slip is shown in Figs. 20a and 21. The experimental accuracy of the slip measurements plotted in the figure was estimated at 0.0001 in. Therefore some scatter of the plotted results was expected. The slip measurements are shown for Sections 1 and 3. Section 1 was inside the shear connected region

whereas Section 3 was in the region without shear connectors.

In general, there is good agreement in the load-slip relationships at similar sections in corresponding beams. The slip curve for beam CC-3F at Section 3 became very flat due to the small amount of reinforcement steel that remained after the fatigue failure of the upper layer of reinforcement. It was observed that the load-slip relationships for the different stages of fatigue loading were not very different up to the 60 kips load level.[4]

The distribution of slip measured along the length of each beam at two load levels is shown in Fig. 21. At the 60 kip load level, Fig. 21 indicates that there is a good agreement between the observed slip distribution in corresponding beams. In each case the slip was measured before the fatigue loading of the continuous beams occurred. At the higher load level some differences in the slip distributions along the length of the beams is efident, although the trends are entirely similar. Large slips occurred in beam CC-3F when the reinforcement bars failed. For beams SC-4S and CC-4F the differences are due to the more flexible slab of the continuous beam caused by the large number of cracks.

Figures 20b and 22 show the observed slab separation.

A very irregular pattern can be observed in the region without shear connectors. This irregular behavior can be attributed to the crack development sequence. For beams SC-4S and CC-4F the slab separation at Section 5 increased rapidly until it stabilized. On the other hand the slab separation at Section 3 behaved irregularly. As the crack sequence progressed the curves followed different trends as expected since the rigid concrete portions were deforming into new patterns.

The distribution of slab separation along the length of the beam is shown in Fig. 20b for five different load levels for beam CC-4F. This is typical of the slab separation behavior. This figure illustrates how the slab and steel beam remain in contact at low levels of load.

The observations on slab slip and separation indicated that:

(1) The beams with a higher steel reinforcement percentage exhibited better symmetry of relative movement at the interface.

(2) The slip for continuous composite beams can be reasonably simulated by simple span beams.

(3) The slab and the steel beam remain in contact at several points within the region without shear connectors for low stages of load. As the load increases the two faces separate except at the center support.

3.6 Cracking Behavior

Figures 23 and 24 show the crack patterns in the concrete slabs of the four beams tested. Fig. 23 shows the crack patterns at the working load level(60 kips) and Fig. 24 shows the crack patterns near the ultimate load. It should be recalled that at the working load level the total tension force in the slabs of the beams was small compared to the tension capacity of the slab. This force was less than that required to initiate cracking of the slab based on a cracking strength of one-tenth the compressive strength of the concrete. The cracks which did occur therefore must have originated from secondary effects such as bending in the slab and stress concentrations at the transverse reinforcement locations and shrinkage. As a consequence only a few irregularly spaced cracks could be expected and indeed that was observed, especially in beams SC-3S and CC-3F as shown in Fig. 23. The shrinkage stresses were large enough to produce cracking of the slab even before loading. In the case of beam CC-4F two fully developed shrinkage cracks plus many edge cracks were evident before testing began. Because of the tensile shrinkage forces in the slab of both continuous beams, a reverse camber of the beam occurred which made it difficult to level the specimen prior to testing without introducing additional cracks in the slab.[4] In order to properly align the continuous beams prior

to fatigue testing, several hundred cycles of small amplitude loading were required. Therefore, prior to the actual fatigue testing and prior to the first static test to the working load level, some cracks were already evident in the slab.[4] The conditions described above were not present to the same degree in the simple span tests, SC-3S and SC-4S. Shrinkage stresses appeared to be smaller in beams SC-3S and SC-4S since no cracks were observed prior to the test. Furthermore, the single span beams were not subjected to cyclic loading. Even so, the crack patterns in beams SC-3S and SC-4S were not greatly different from those in the corresponding beams, CC-3F and CC-4F.

The crack patterns in the slabs of the four beams are shown in Fig. 24 near the ultimate load. The similarity of the crack patterns in corresponding beams is much more evident, especially for beams SC-4S and CC-4F.

Of significance is the marked difference in cracking behavior between the beams having the smaller (0.61%) amount of steel reinforcement (SC-3S and CC-3F) and those with higher (1.02%) amounts of steel reinforcement (SC-4S and CC-4F). For continuous beams CC-3F and CC-4F the fatigue loading increased the number of cracks in the slab. All cracks for beam CC-3F were developed during the fatigue test, as well as most of the cracks for beam CC-4F. Simple beams SC-3S and SC-4S had additional cracks develop

with the load increments beyond the working load level. In beam SC-3S these cracks occurred at a small increment of the load over the working load level. Afterwards the number of cracks (seven) remained constant until the ultimate load was reached and a large plastic deformation occurred in the steel beam when two additional cracks developed. The beams with the small amount of reinforcement steel did not develop a large number of cracks. However, the width of the cracks increased markedly from initial loading until the ultimate load was reached. This was not the case for beams SC-4S and CC-4F where the individual crack width did not increase significantly, but many more cracks developed as is evident by comparing Figs. 23 and 24.

The difference in the cracking behavior described above was due to early yielding of the longitudinal reinforcement in beams SC-3S and CC-3F which prevented the development of a larger slab force. Yielding in the reinforcing bars occurred at a load level of about 80 kips which was 30% above the working load level. Thus the yield stress level in the reinforcement was reached much earlier than would be predicted by simple tie-bar theory (See Fig. 18a), where yielding for the bars was expected to occur at ultimate load. Yielding occurred at the crack locations next to the center line.

It should be pointed out that the ultimate tension

capacity of the concrete slab for beams SC-3S and CC-3F was larger than the yield capacity of the longitudinal reinforcement bars. On the other hand, the stresses in the reinforcement for beams SC-4S and CC-4F remained below the yield stress level until the ultimate load was reached. Up to that point the cracks closed almost completely upon removal of load. For beams SC-4S and CC-4F the yield capacity of the reinforcement exceeded the ultimate tension capacity of the slab.

Figure 25 shows histograms of crack width versus frequency of occurrence for the four test beams. All of the measured crack widths for loads ranging from zero to the working load level were included. The effect of including all measured crack widths was to spread out the histograms over a wider range of crack widths, without altering the position of the mean and maximum crack widths. This procedure was desirable since the crack widths were influenced not only by the load level but also by new crack developments. The ACI recommended maximum crack width for exterior members is also shown in Fig. 25. It can be observed that much more desirable cracking behavior was evident in beams SC-4S and CC-4F which had the larger amount of longitudinal steel reinforcement.

From the above discussion it can be concluded that:

(1) Beams SC-3S and CC-3F with 0.61% longitudinal

reinforcement exhibited an undesirable crack pattern of a few widely spaced cracks of large width. The cracking behavior of beams SC-4S and CC-4F with 1.02% longitudinal reinforcement was much more desirable. Cracks were much smaller, much more frequent, and more evenly distributed.

(2) The very similar cracking behavior exhibited by corresponding beams indicated that the cracking behavior of continuous composite beams in the negative moment region can be simulated by simple span beams under negative moment.

3.7 Failure Mode

Figure 26 shows a typical simple span beam after ultimate load was reached and all instrumentation removed. The figure clearly shows the large deformation which occurred during the test, reaching 4 to 6 in. at the load point for the beam. In both simple span test beams and in the two continuous beams failure eventually occurred after the lower flange of the steel beam had buckled next to the center support as can be seen in Fig. 27.

Local buckling usually occurred only after the ultimate load capacity was reached and large deformations occurred. An exception was in test beam SC-4S, where local buckling occurred

almost simultaneously with the ultimate load (Fig. 19b). The observed mode of failure therefore was similar to that exhibited by the continuous beams reported in Ref. 4 where the same cross-section was used.

4. SUMMARY AND CONCLUSIONS

Two simply supported composite steel-concrete beams were tested statically under negative bending moment conditions (slab in tension). These beams were designed to simulate the negative moment region of two, two-span continuous composite beams having spans of 25'-0" which were tested under fatigue and static loading. The results of those tests are reported elsewhere.[4] Each of the simple span beams reported herein had span lengths of 12'-8". The cross-sections were identical with a 6"x60" reinforced concrete slab connected to a W21x62 rolled steel beam by means of 4" high 3/4" diameter headed steel studs. These studs were concentrated near the support points of the beams. One beam was designed with 0.61% longitudinal reinforcement in the slab. This amount of reinforcement was determined by the present AASHO Provisions for distribution reinforcement. The other beam was designed with 1.02% longitudinal reinforcement in the slab. The distribution of stud shear connectors was the same in each beam although a greater number of studs were required in the beam with the 1.02% slab reinforcement.

The results of these static tests were presented in this report. The following conclusions can be made:

(1) The observed comparative behavior of the two test

beams, as well as the analysis of the test data indicated that a more satisfactory structural behavior was achieved by the test beam having the higher percentage (1.02%) of longitudinal slab reinforcement. The behavior of this beam was characterized by a lower and more predictable stress level in the longitudinal reinforcement (important from fatigue considerations), and a more satisfactory crack pattern in the slab with smaller crack widths.

(2) The test results indicated that to achieve a satisfactory cracking behavior in the slab, the strength of the longitudinal reinforcement should exceed the tensile strength of the concrete. In the tests reported herein, the beam with the lower steel percentage (0.61%) did not meet this condition whereas the other beam (1.02%) did.

(3) The test results indicated that a satisfactory simulation of the negative moment region was achieved within the scope of this study. Therefore, future tests of the type could be used to study negative moment regions of continuous composite beams more easily and economically.

(4) Existing methods of analysis (simple tie-bar

theory, complete and partial interaction theory) do not accurately predict the stresses in the reinforced concrete slab. Additional research is required to develop a more rational method of analysis.

5. ACKNOWLEDGMENTS

The study described in this report was part of an investigation on composite beams that was conducted at Fritz Engineering Laboratory, Department of Civil Engineering, Lehigh University. L. S. Beedle is Director of Fritz Engineering Laboratory and D. A. VanHorn is Chairman of the Department of Civil Engineering. The project was sponsored by the Pennsylvania Department of Transportation and the Federal Highway Administration.

The writers wish to thank Dr. R. G. Slutter for his advice and help in the planning and conduct of these tests, and to Messrs. K. R. Harpel and H. Sutherland and their staff at the Fritz Laboratory for their work in preparing the test set-up and instrumentation; to R. N. Sopko and his staff for preparing drawings and providing the photographic coverage; to Mr. M. Karim for assistance in the preparation of the manuscript of this report; and to Mrs. Charlotte Yost for typing the manuscript.

6. TABLES AND FIGURES

TABLE 1

MECHANICAL PROPERTIES OF STEEL

Type of Specimen	No. of Test	Yield Point (KSI)	Static Yield Stress (KSI)	Tensile Strength (KSI)
		Mean	Mean	Mean
Web W21x62	12	37.5	35.5	62.7
Flange W21x62	12	35.9	34.1	61.4
No. 4 Bar	5		46.0	76.1
No. 5 Bar	8		44.	72.5

TABLE 2

RESULTS OF CONCRETE CYLINDER TESTS

Standard Test				Cylinders Cured With Slab	
Beam	Tensile Strength (psi)	f'_c Compressive Strength (psi)	Modulus of Elasticity (ksi)	Tensile (psi)	Compressive (psi)
SC-3S	586	4690	3471	533	4580
SC-4S	587	5430	3940	530	4050

TABLE 3

ROLLED STEEL BEAM PROPERTIES

BEAM	AREA $(in)^2$	DEPTH (in)	FLANGE		WEB THICKNESS (in)	MOMENT OF INERTIA $(in)^4$
			WIDTH (in)	THICKNESS (in)		
SC-3S	17.474	20.955	8.366	0.546	0.407	1245.354
SC-4S	17.633	20.986	8.257	0.561	0.415	1257.056
*W21x62	18.230	20.990	8.250	0.615	0.400	1327.000

* From AISC Manual of Steel Construction

TABLE 4

PROPERTIES OF THE TEST BEAMS

BEAM	AREA OF REINFORCEMENT TOP LAYER $in.^2$	AREA OF REINFORCEMENT BOTTOM LAYER $in.^2$	MOMENT OF INERTIA TRANSFORMED SECTION $in.^4$	MOMENT OF INERTIA STEEL SECTION* $in.^2$	COMPUTED ULTIMATE MOMENT kip-in.
SC-3S	1.20	1.00	3745	1685	6030
SC-4S	2.75	1.00	3797	1900	6873

* Including Reinforcement Steel

TABLE 5

FORCE ON THE SHEAR CONNECTORS

Load	Theory for SC-3S CC-3F	Test Results				Theory for SC-4S CC-4F	Test Results			
		SC-3S	CC-3F				SC-4S	CC-4F		
			10 cyls.	600 KCyls.	2000 KCyls.			10 cyls.	600 KCyls.	2000 KCyls.
Kips	Kips	Kips	Kips	Kips	Kips	Kips	Kips	Kips	Kips	Kips
60	1.95	2.91	3.41	4.14	2.14	2.72	6.34	5.61	4.24	4.44
100	3.25	8.09				4.55	6.43			5.80
150	9.02	9.00				7.12*	7.40*			8.61

* number of connectors estimated as 13 (first row of connectors of the support line included)

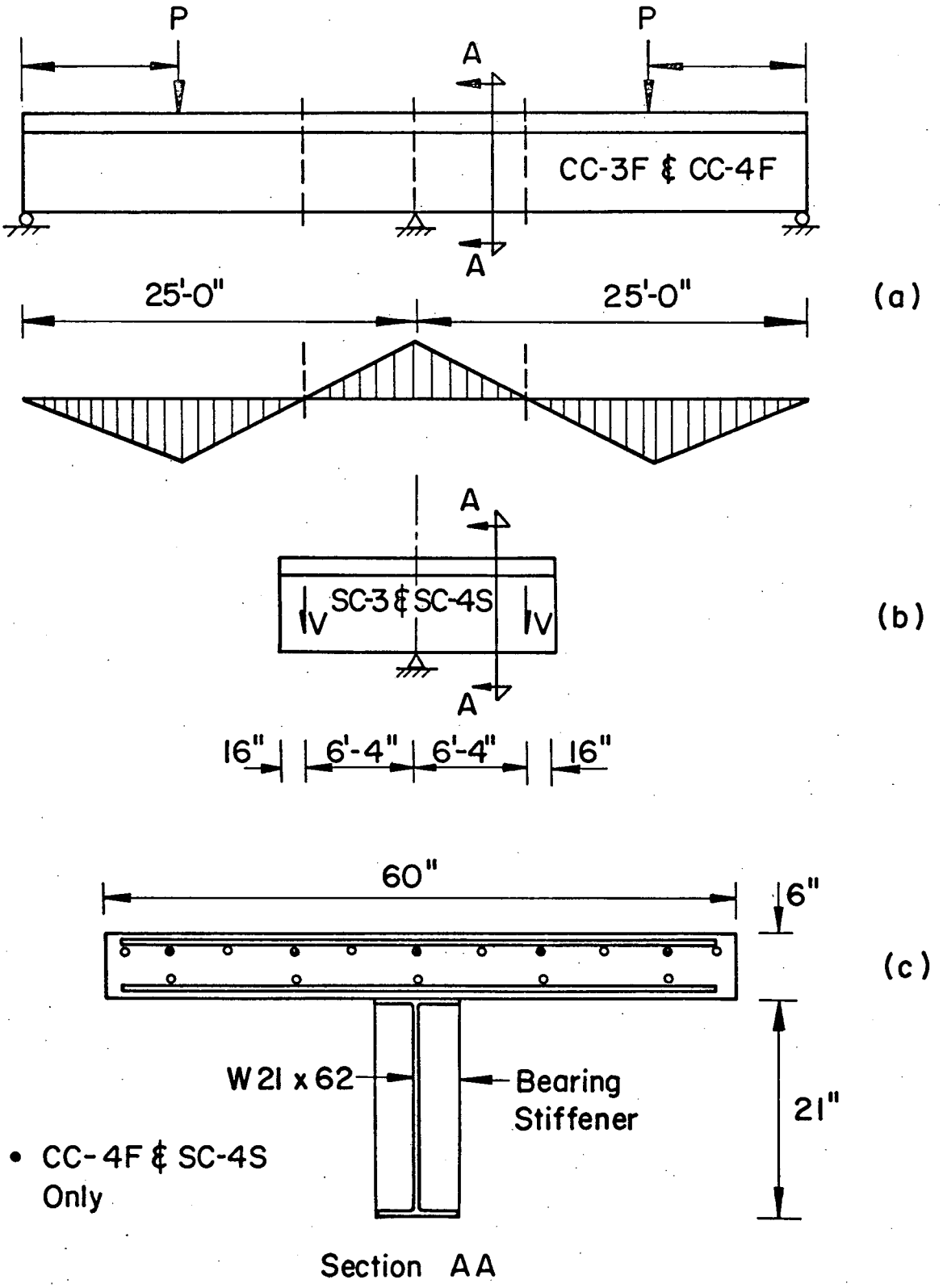

FIG. 1 TEST BEAMS

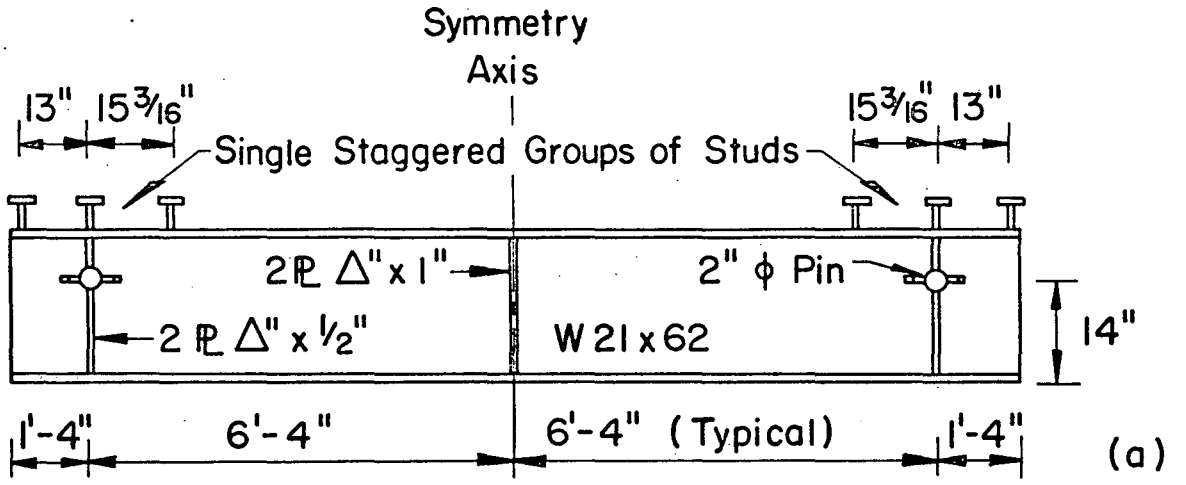

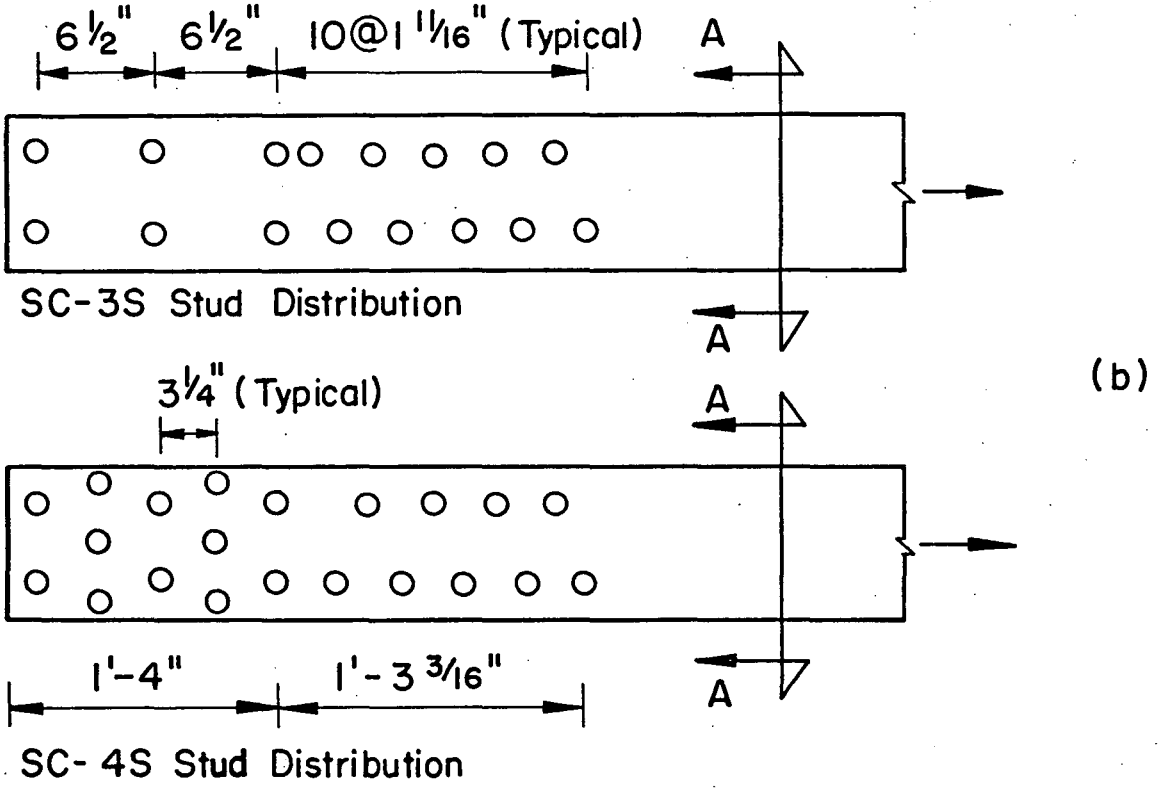

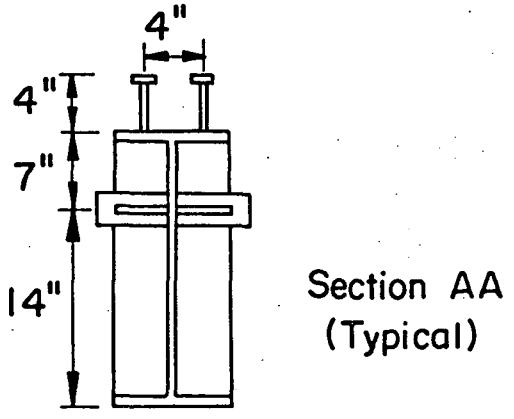

FIG. 2 FABRICATION DETAILS

(a)

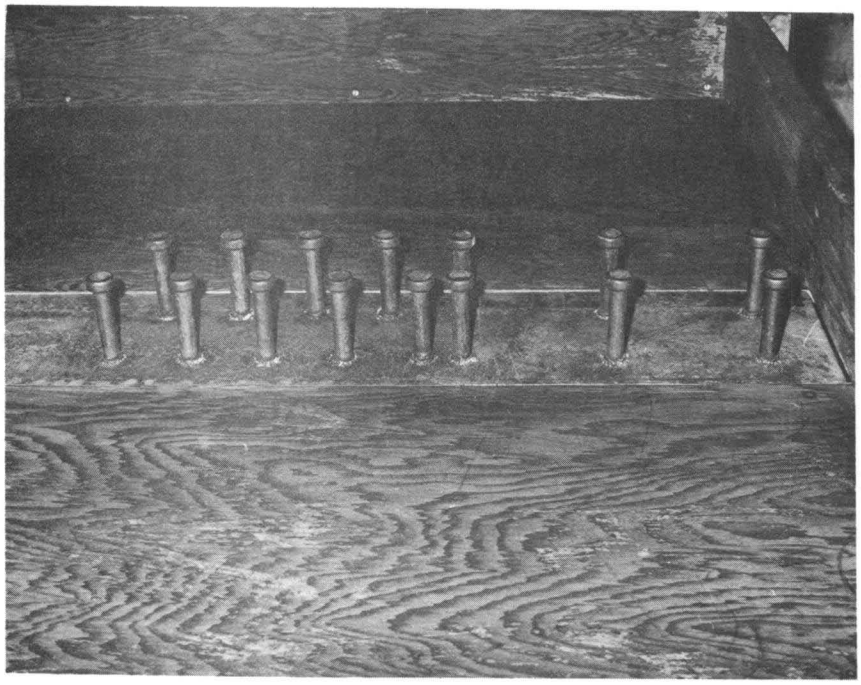

(b)

FIG. 3 FORMWORK

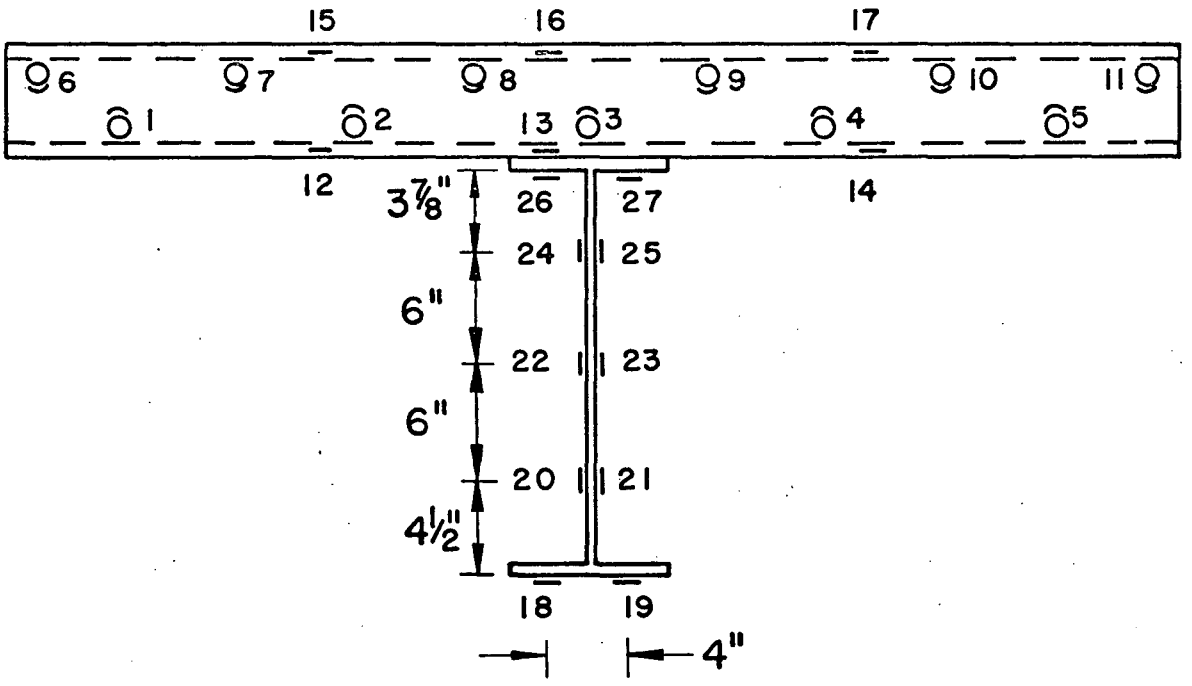

FIG. 4 CROSS SECTIONAL STRAIN GAGE DISTRIBUTION

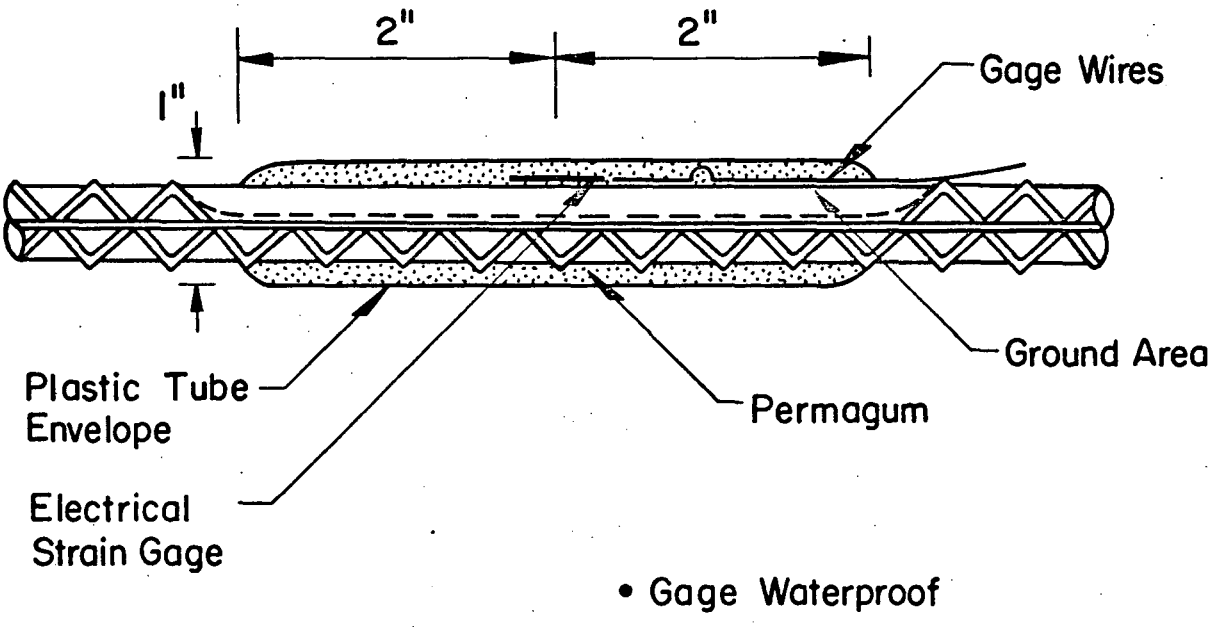

FIG. 5 STRAIN GAGE PROTECTION

(a)

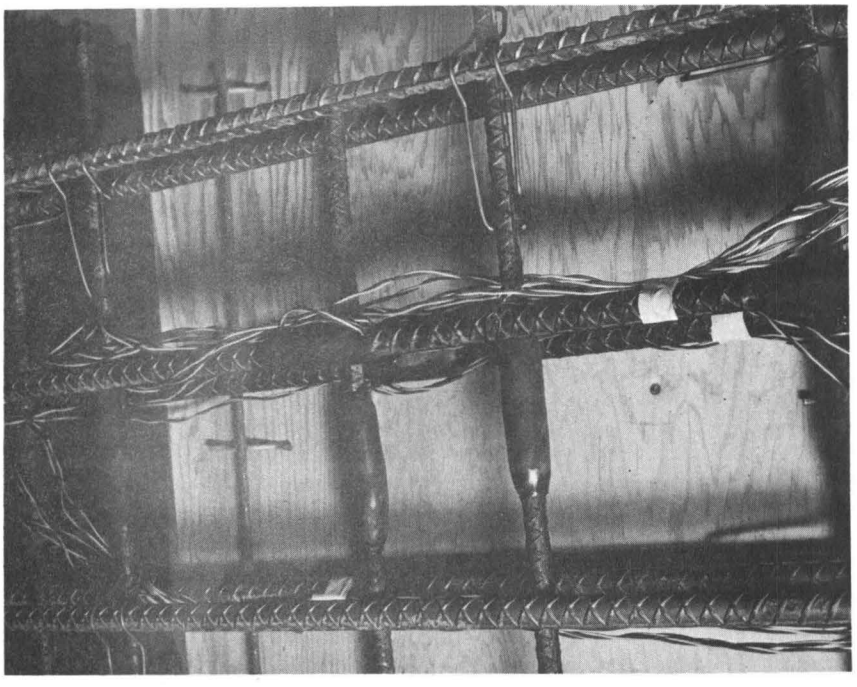

(b)

FIG. 6 INSTRUMENTATION DETAILS

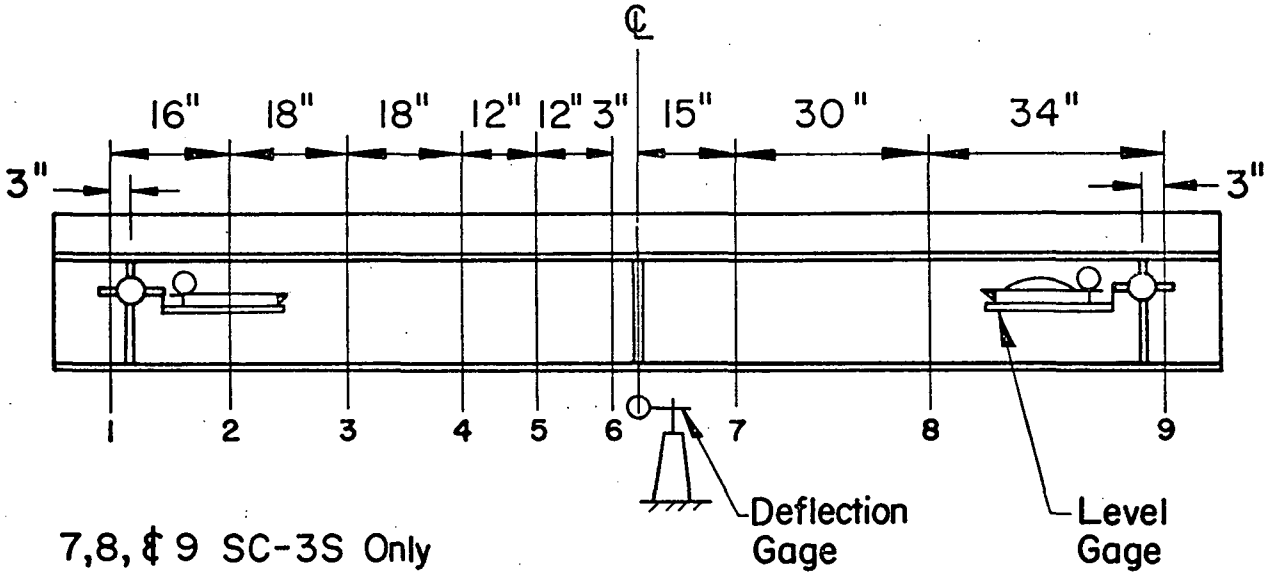

FIG. 7 INSTRUMENTED CROSS SECTIONS FOR SC-3S, SC-4S TEST BEAMS

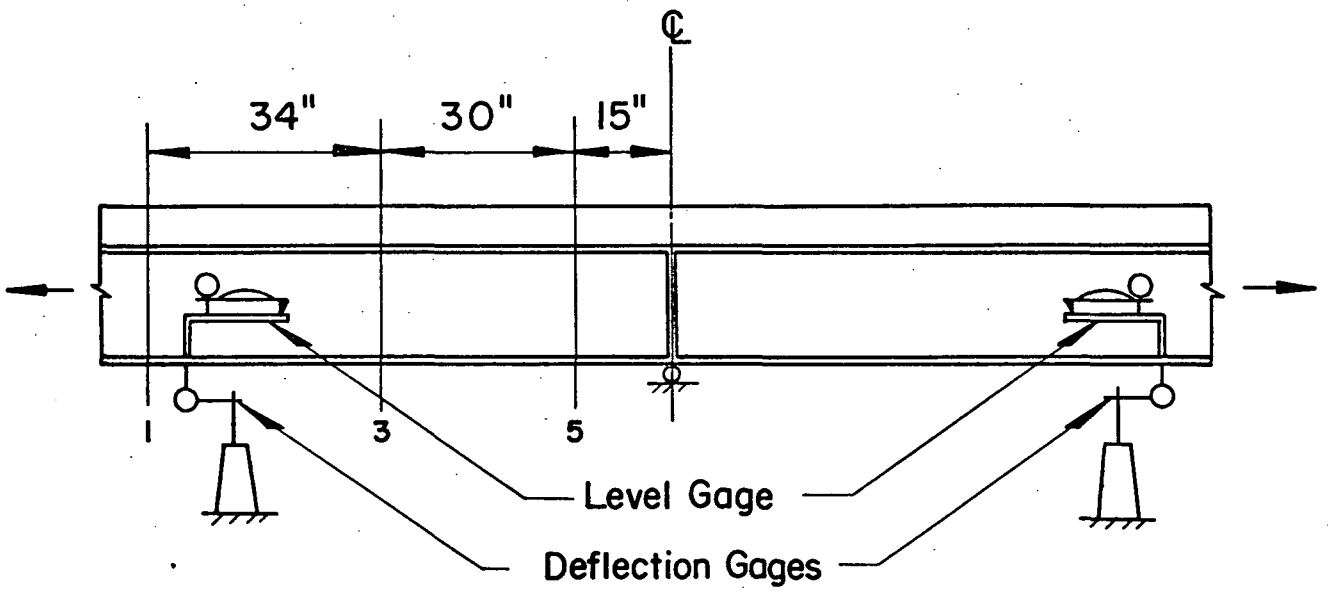

FIG. 8 INSTRUMENTED CROSS SECTIONS FOR CC-3F & CC-4F TEST BEAMS

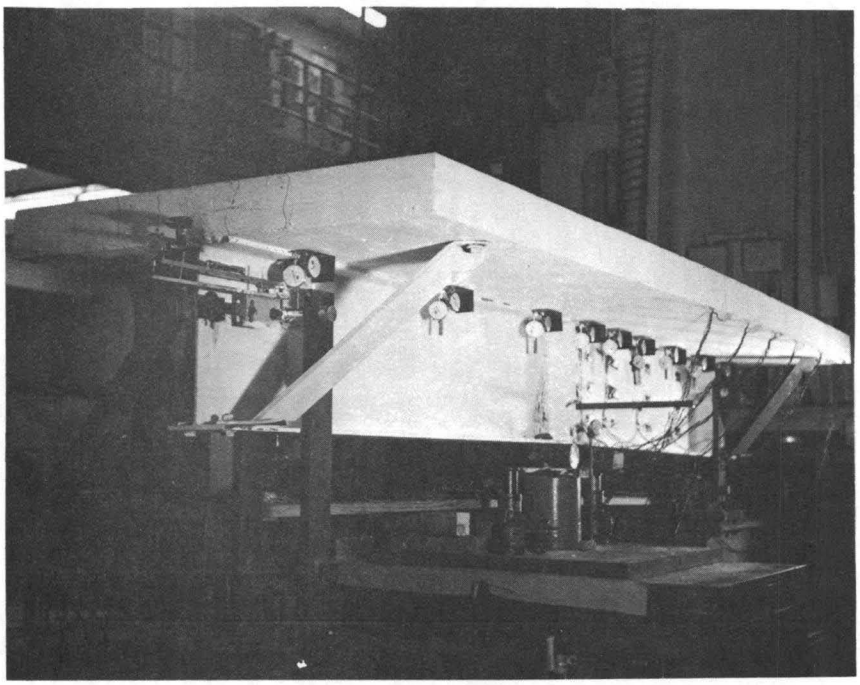

FIG. 9 TEST SET UP

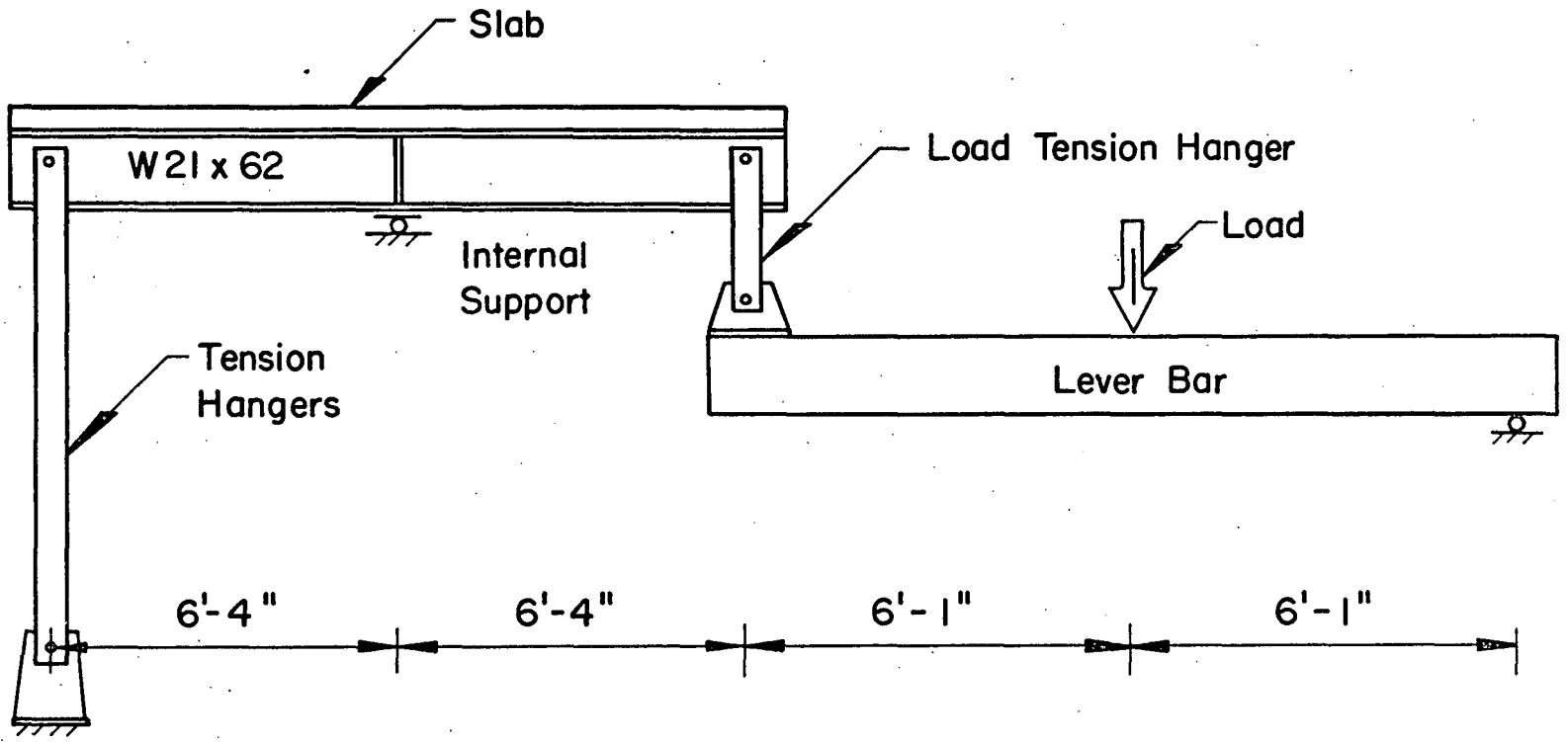

FIG. 10 NEGATIVE MOMENT BENDING TEST SET UP

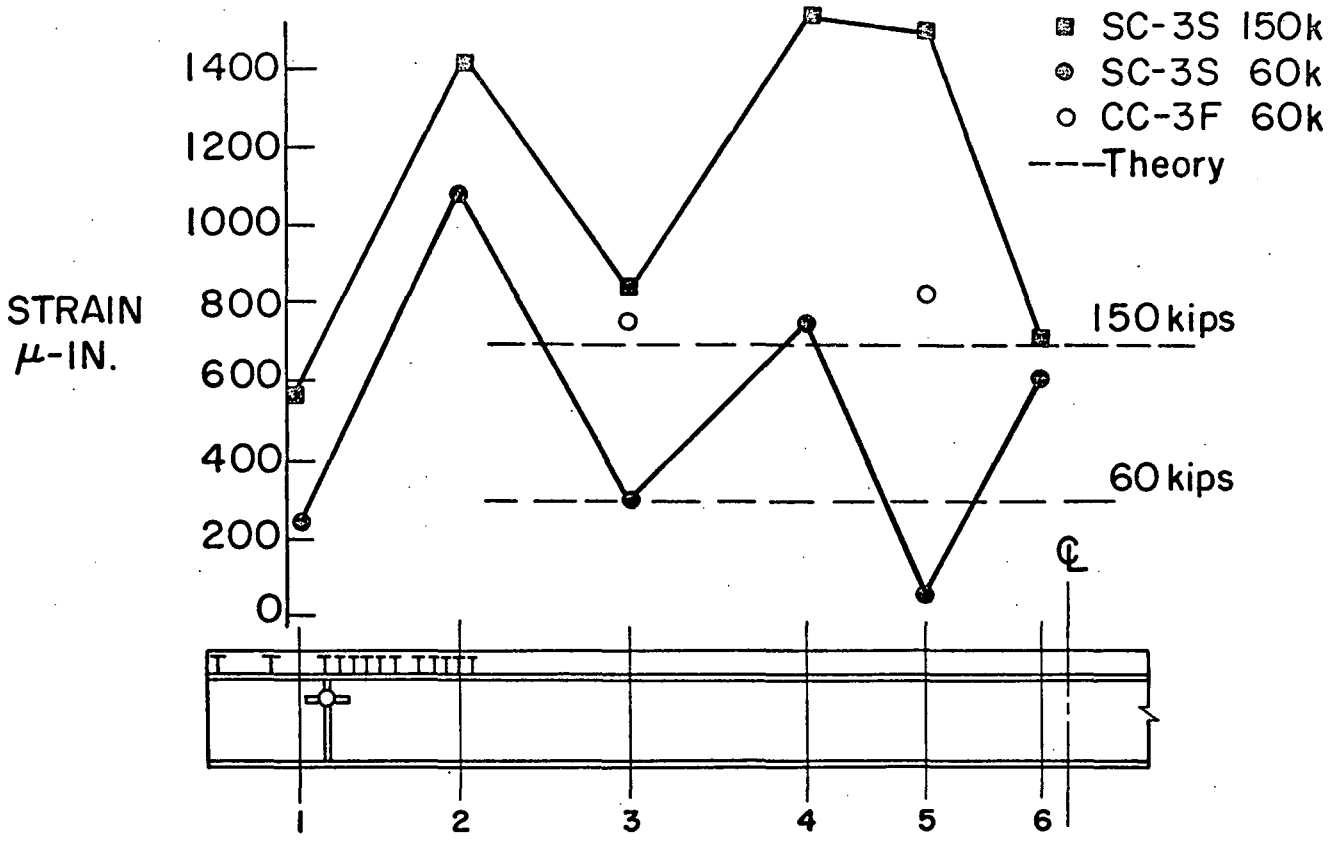

(a) Beam SC-3S

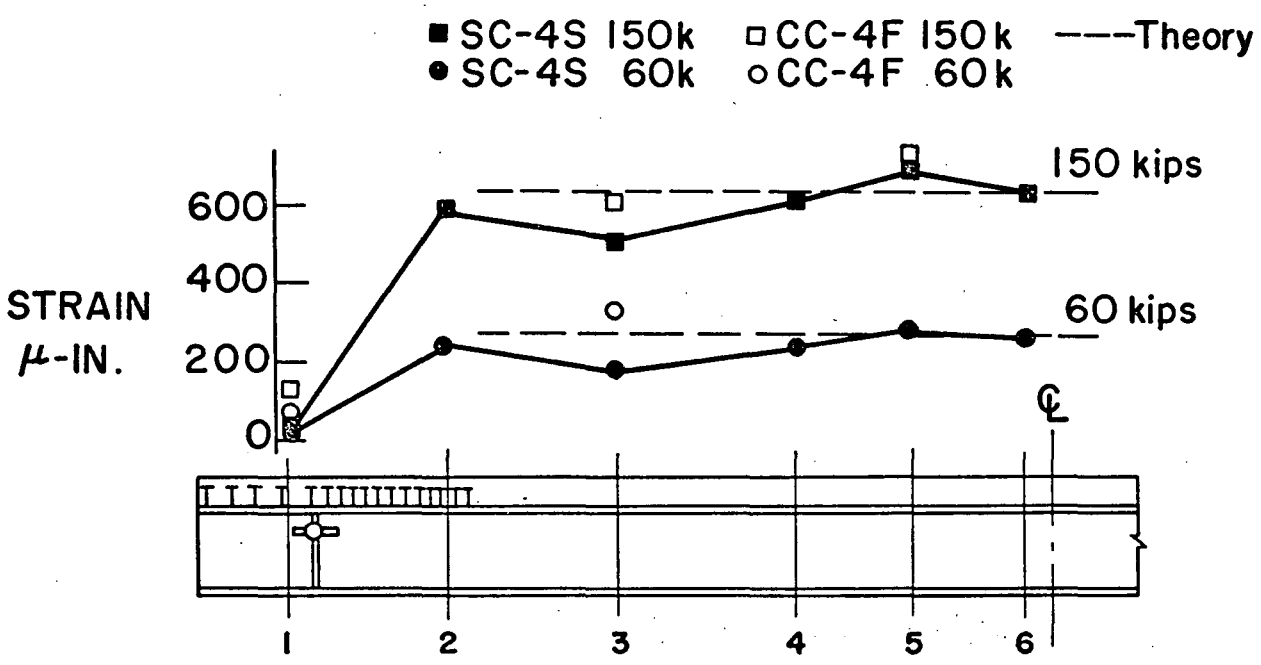

(b) Beam SC-4S

FIG. 11 AVERAGE STRAIN DISTRIBUTION IN THE LONGITUDINAL SLAB REINFORCEMENT

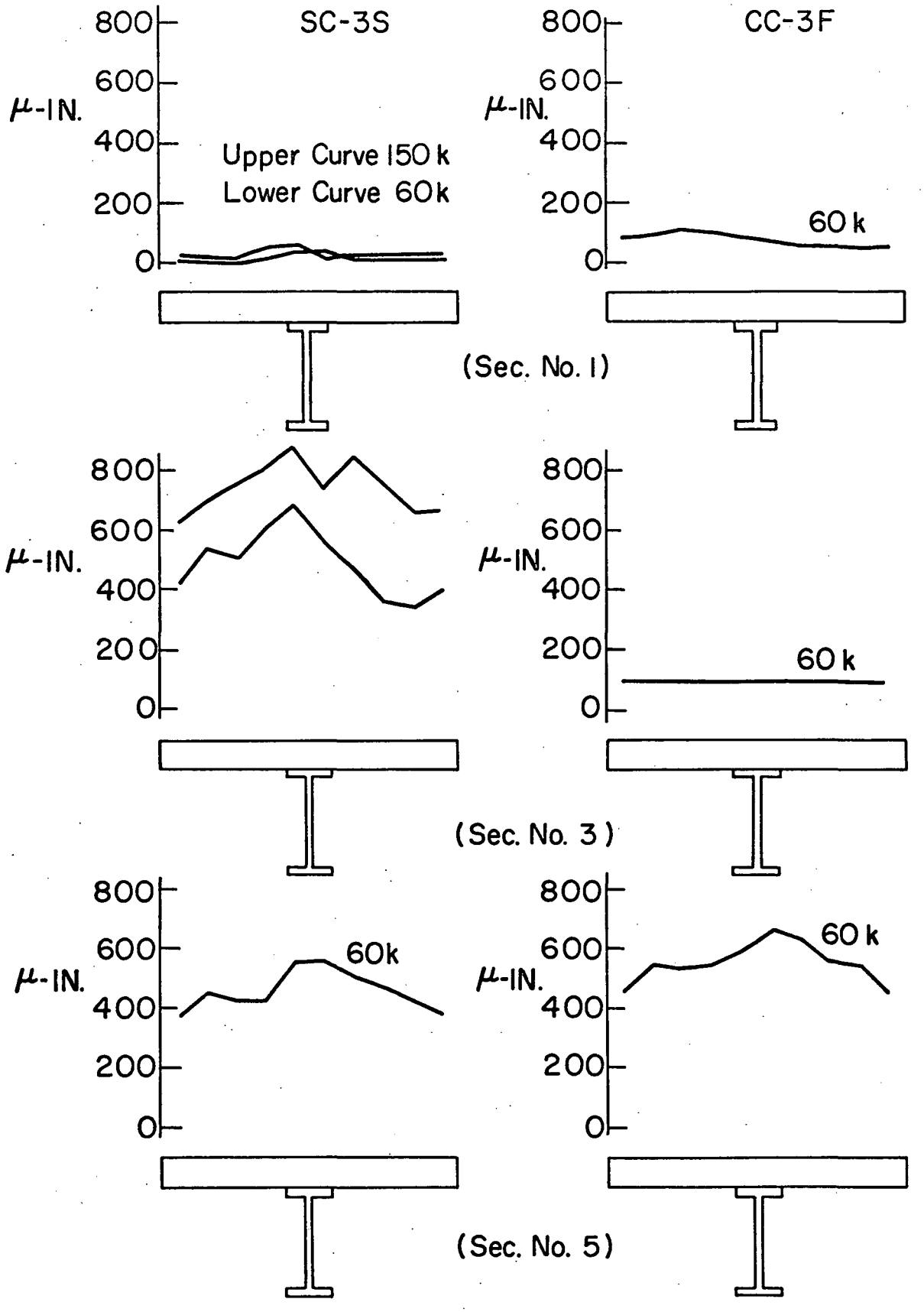

FIG. 12 LONGITUDINAL MID-DEPTH STRAIN DISTRIBUTION

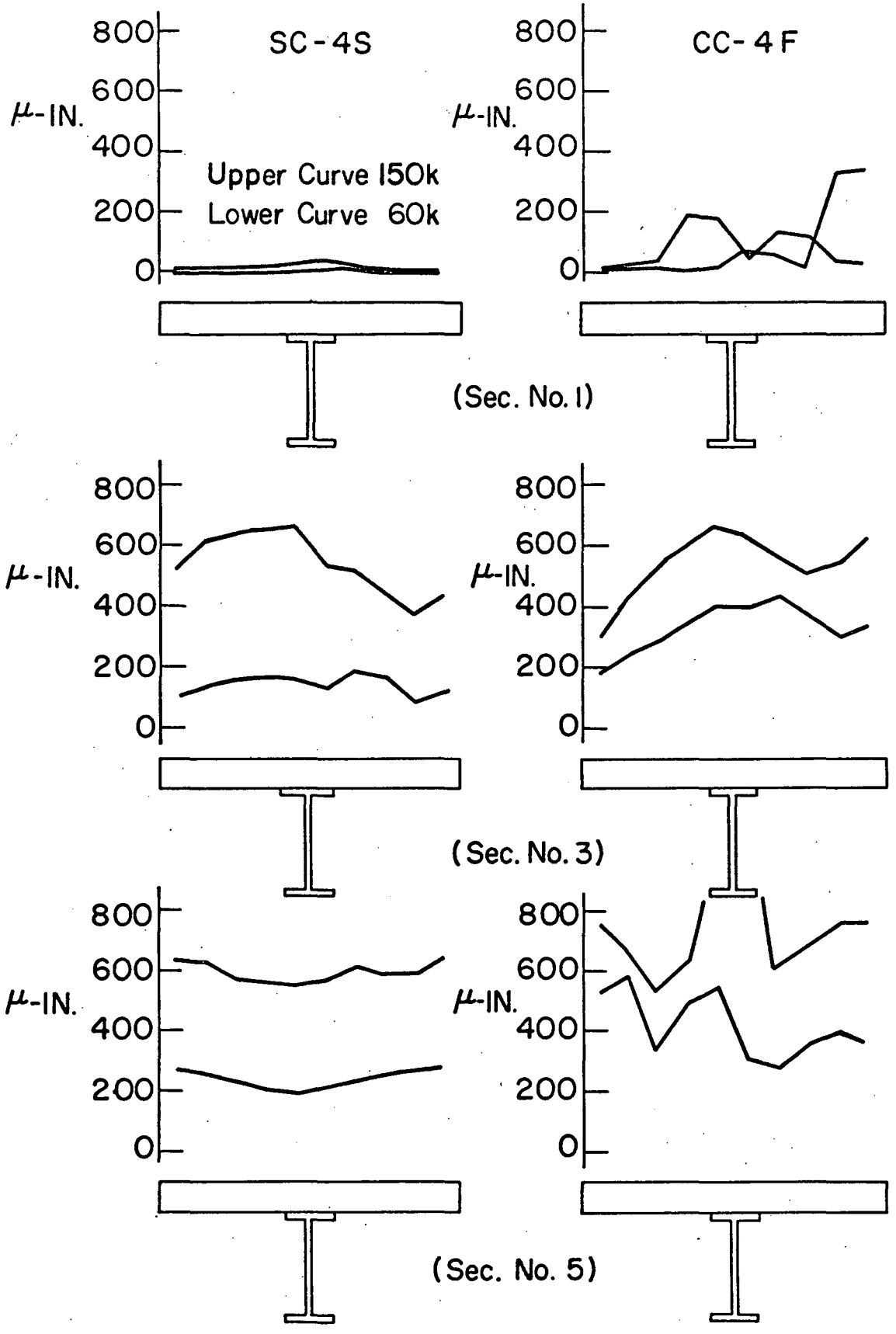

FIG. 13 LONGITUDINAL MID-DEPTH STRAIN DISTRIBUTION

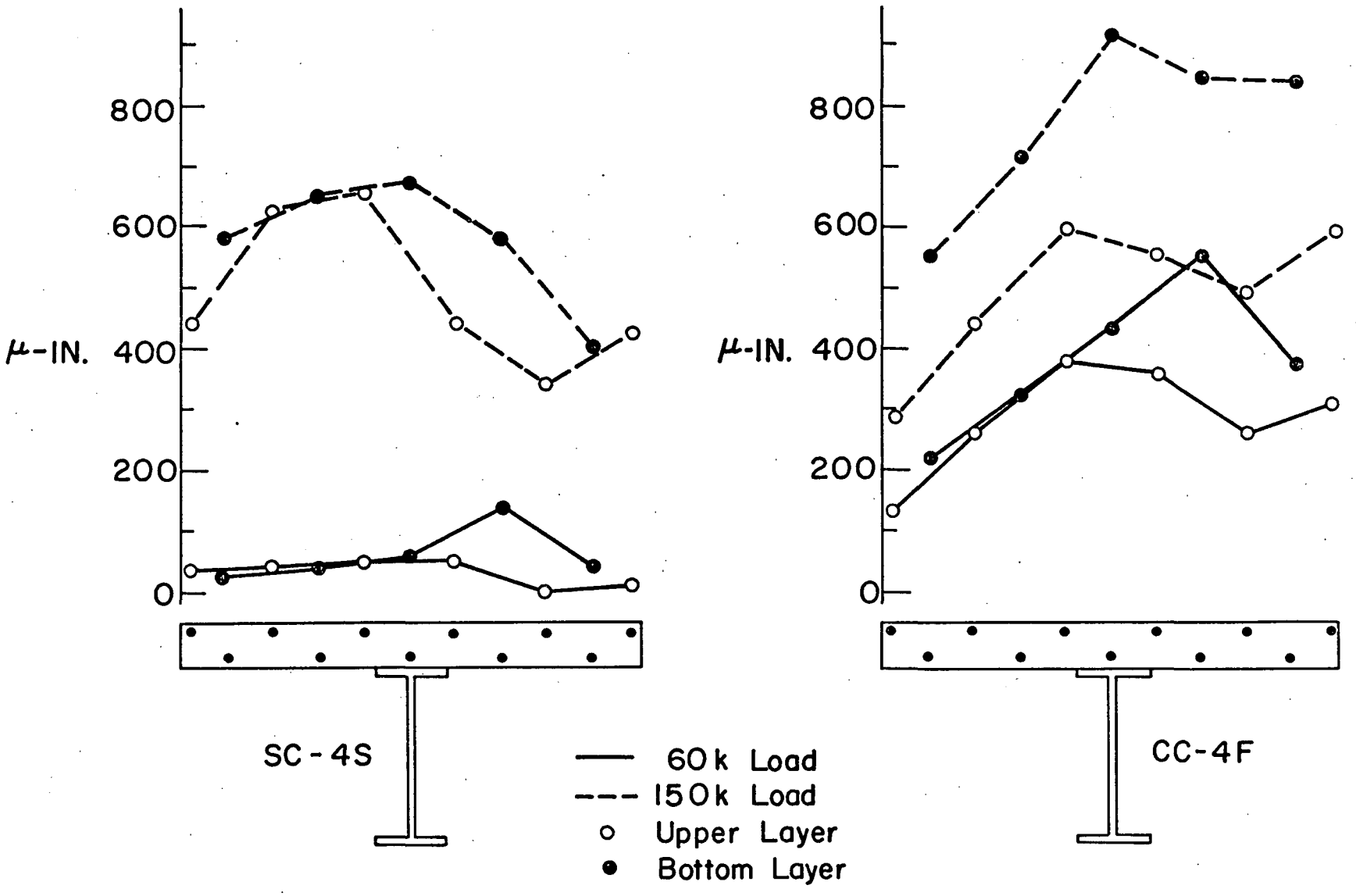

FIG. 14 STRAIN DISTRIBUTION FOR SECTION 3 BEAMS SC-4S & CC-4F

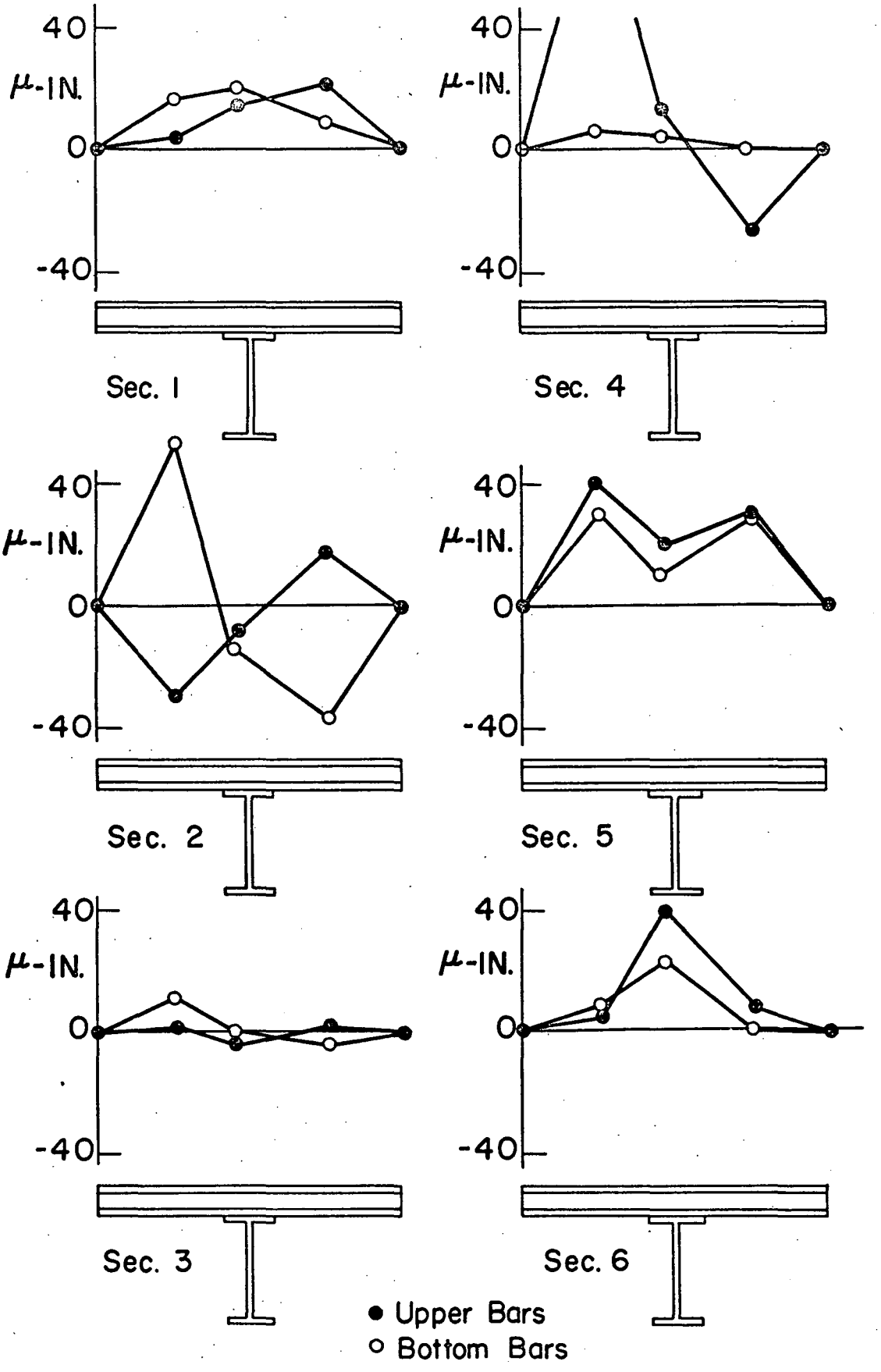

FIG. 15 TRANSVERSAL STEEL STRAINS FOR BEAM SC-4S

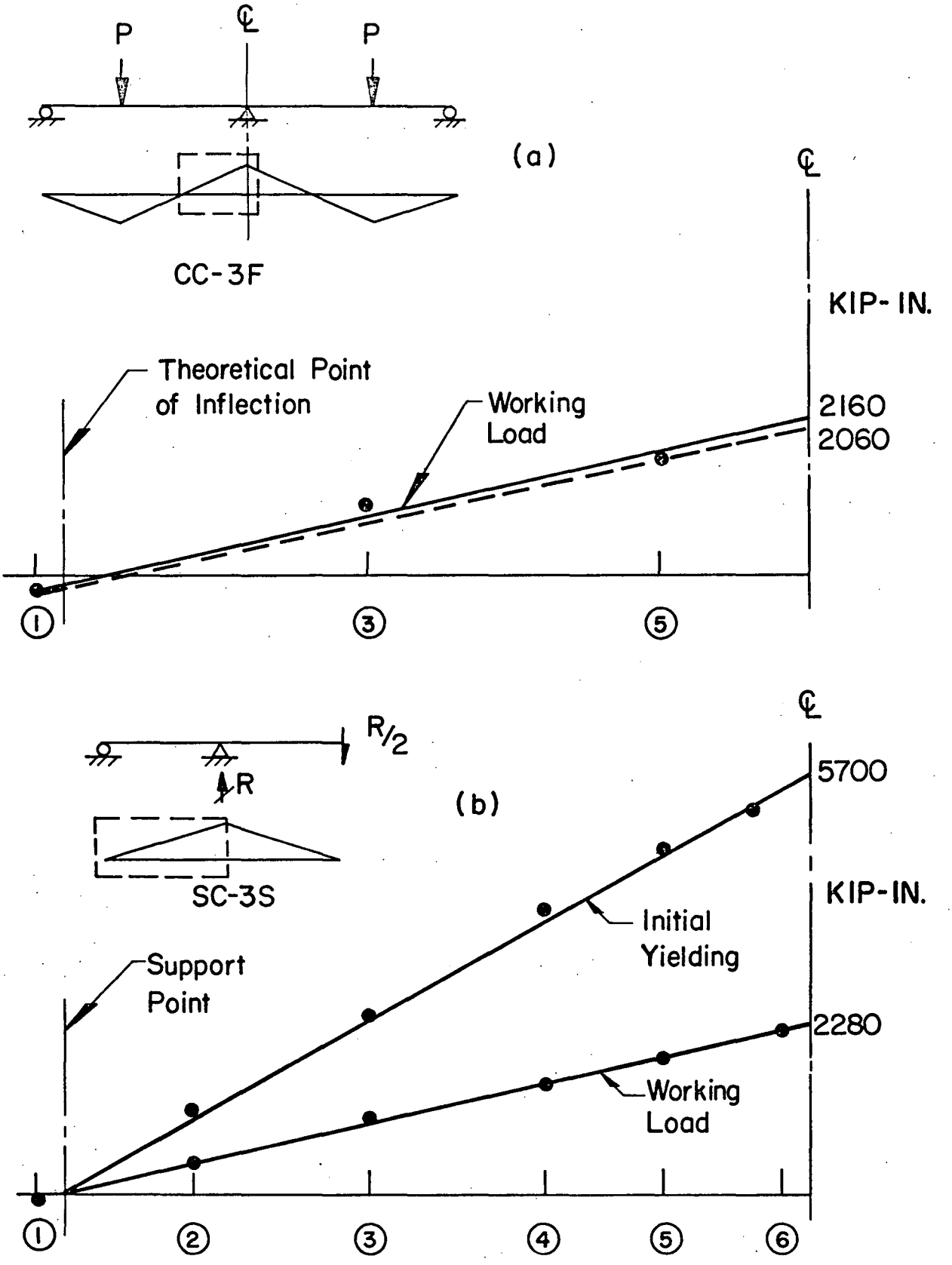

FIG. 16 NEGATIVE BENDING MOMENT DISTRIBUTION

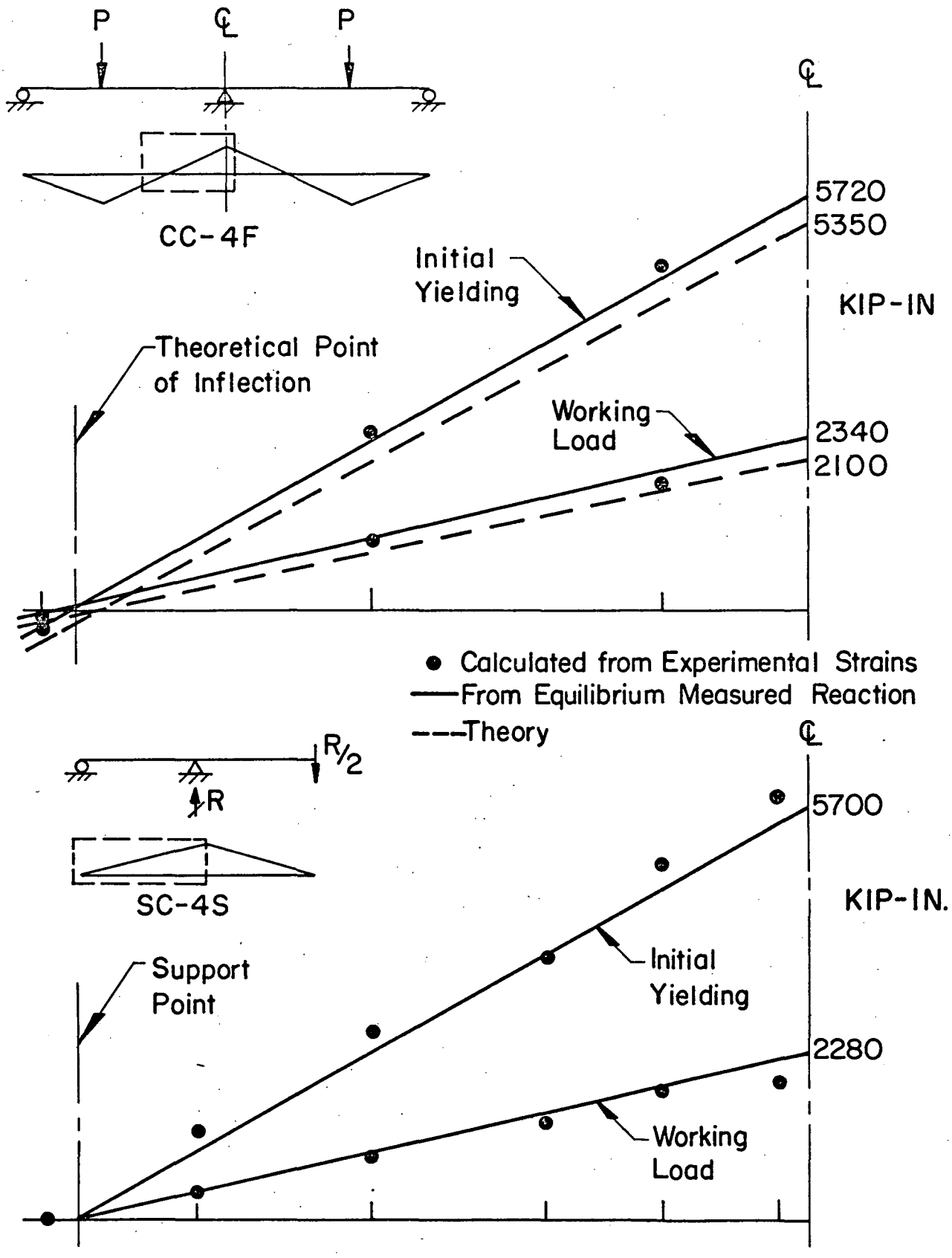

FIG. 17 NEGATIVE BENDING MOMENT DISTRIBUTION

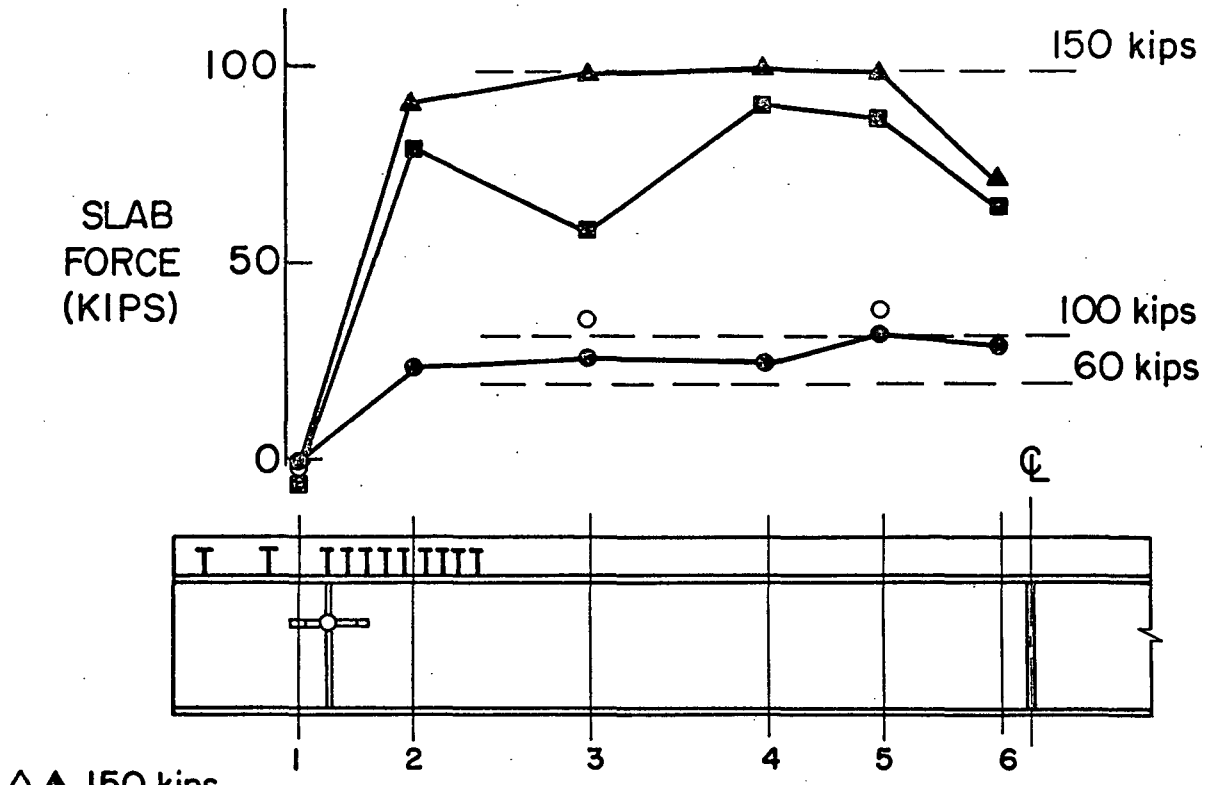

△ ▲ 150 kips
□ ■ 100 kips
○ ● 60 kips

(a) Beam SC-3S

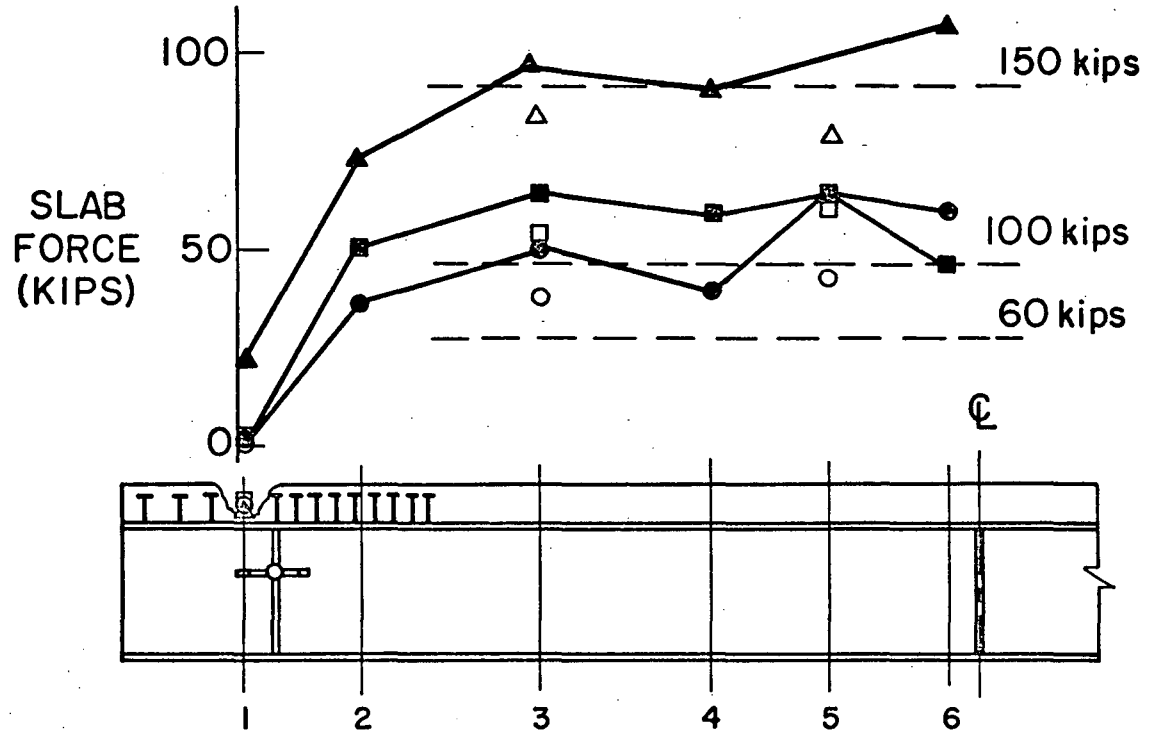

(b) Beam SC-4S

FIG. 18 FORCE DISTRIBUTION IN SLAB

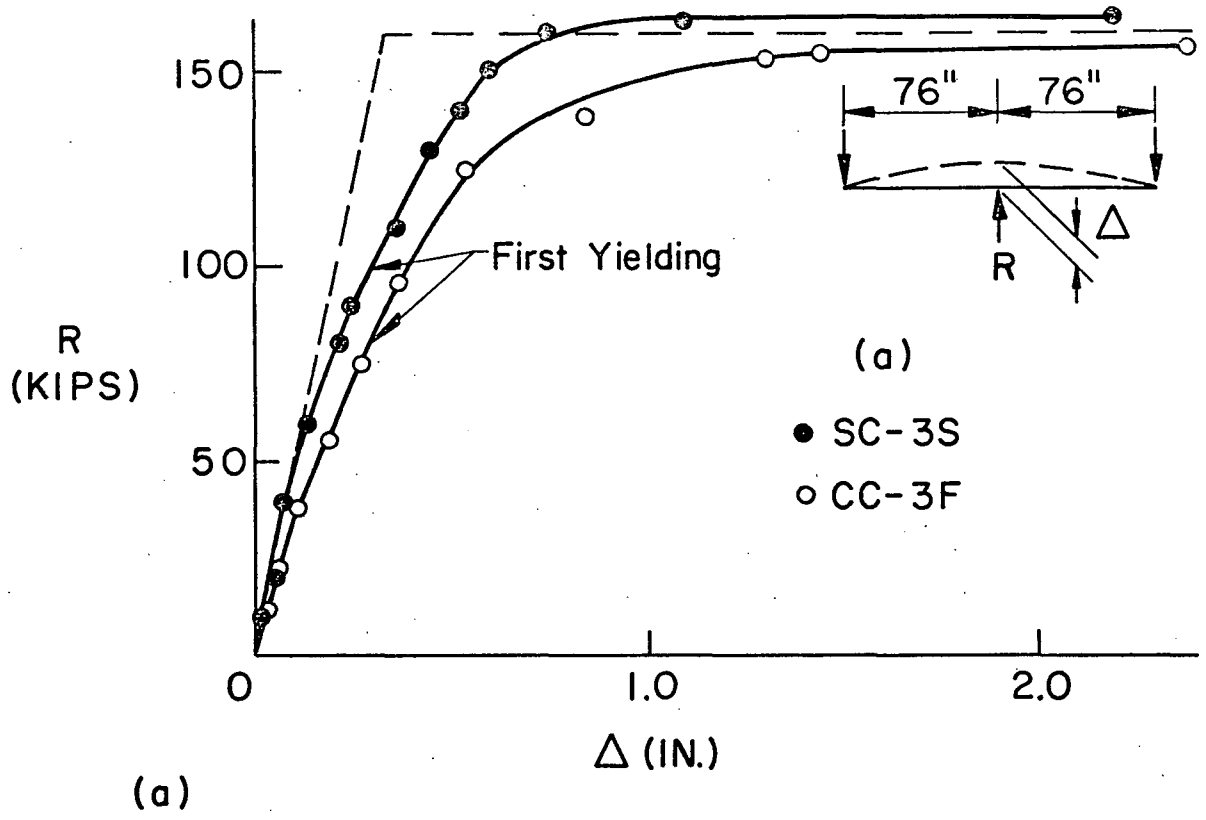

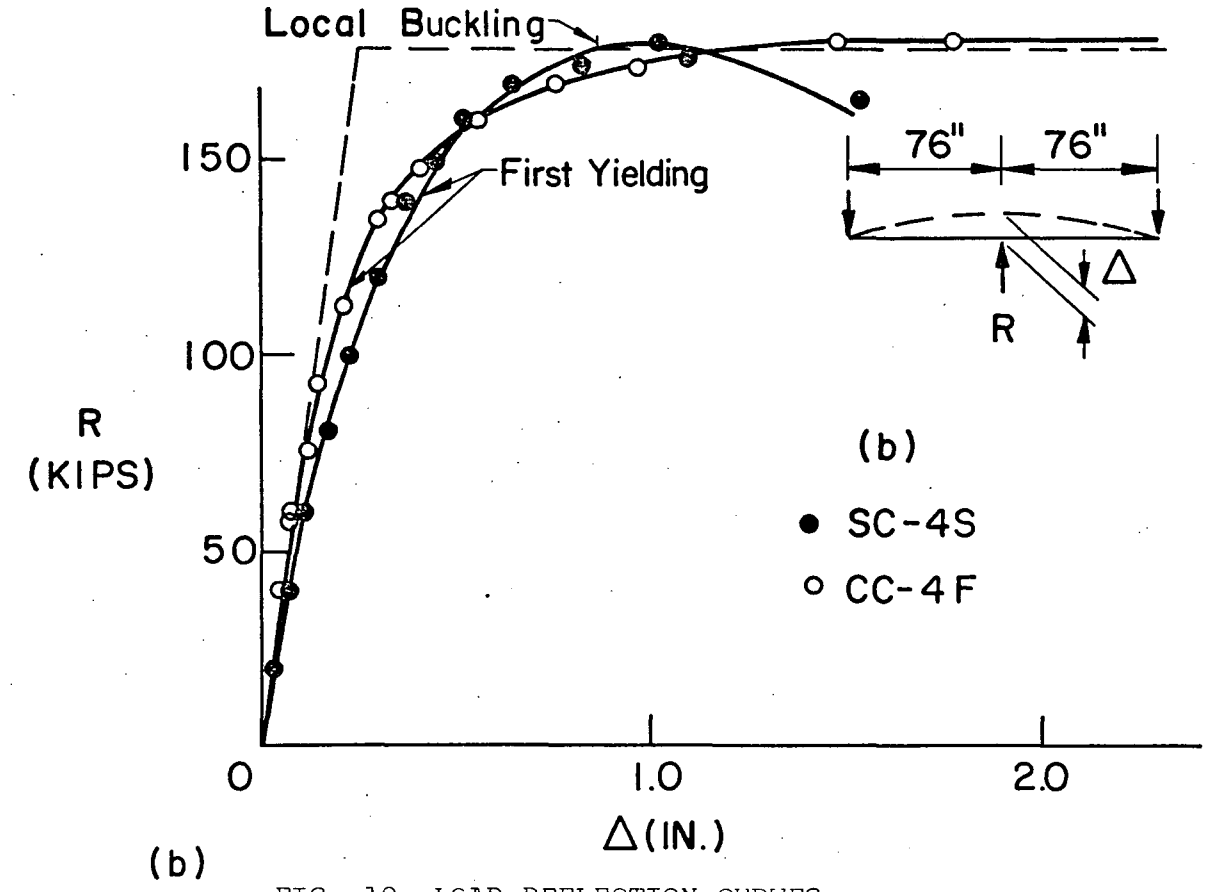

FIG. 19 LOAD DEFLECTION CURVES

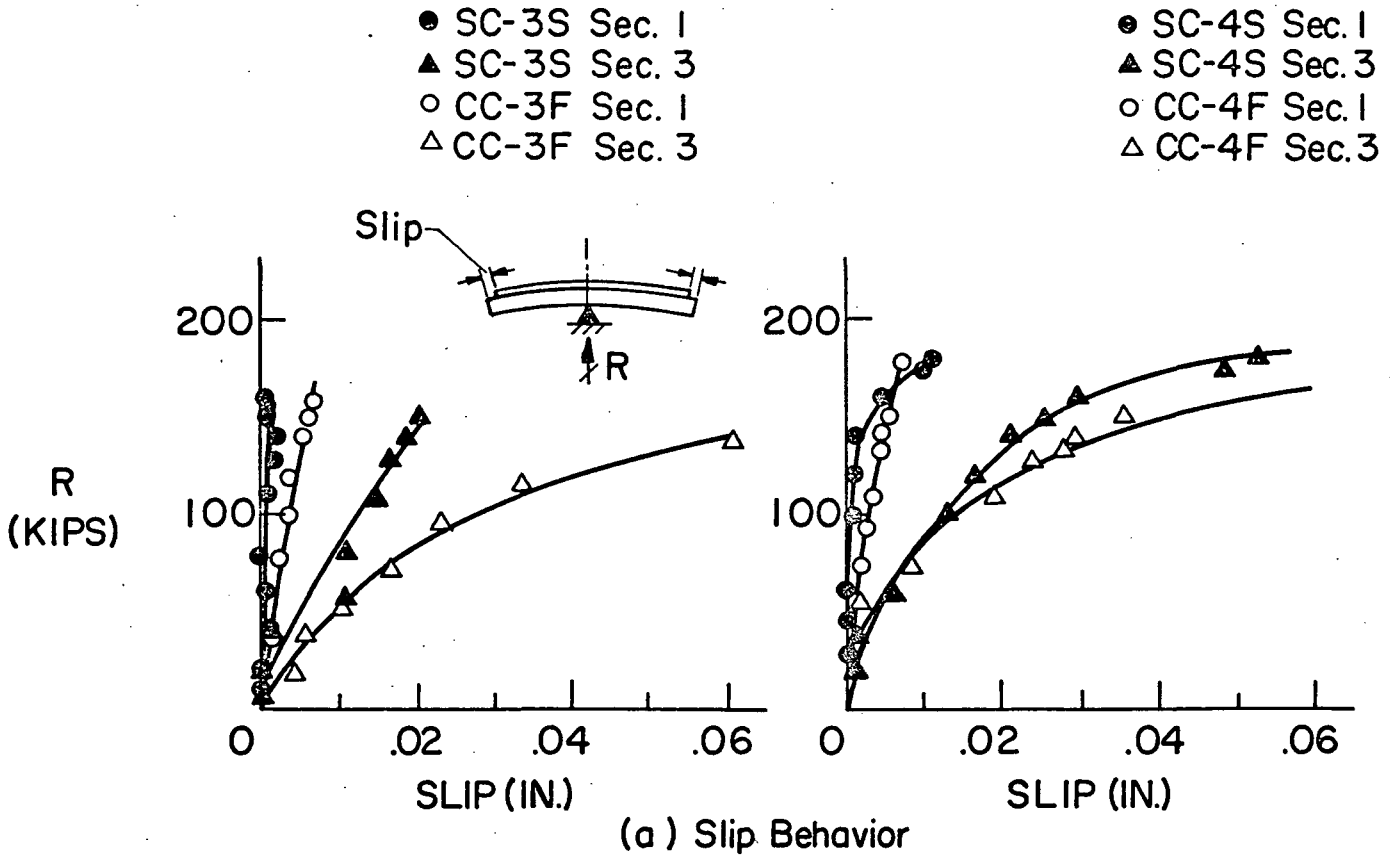

(a) Slip Behavior

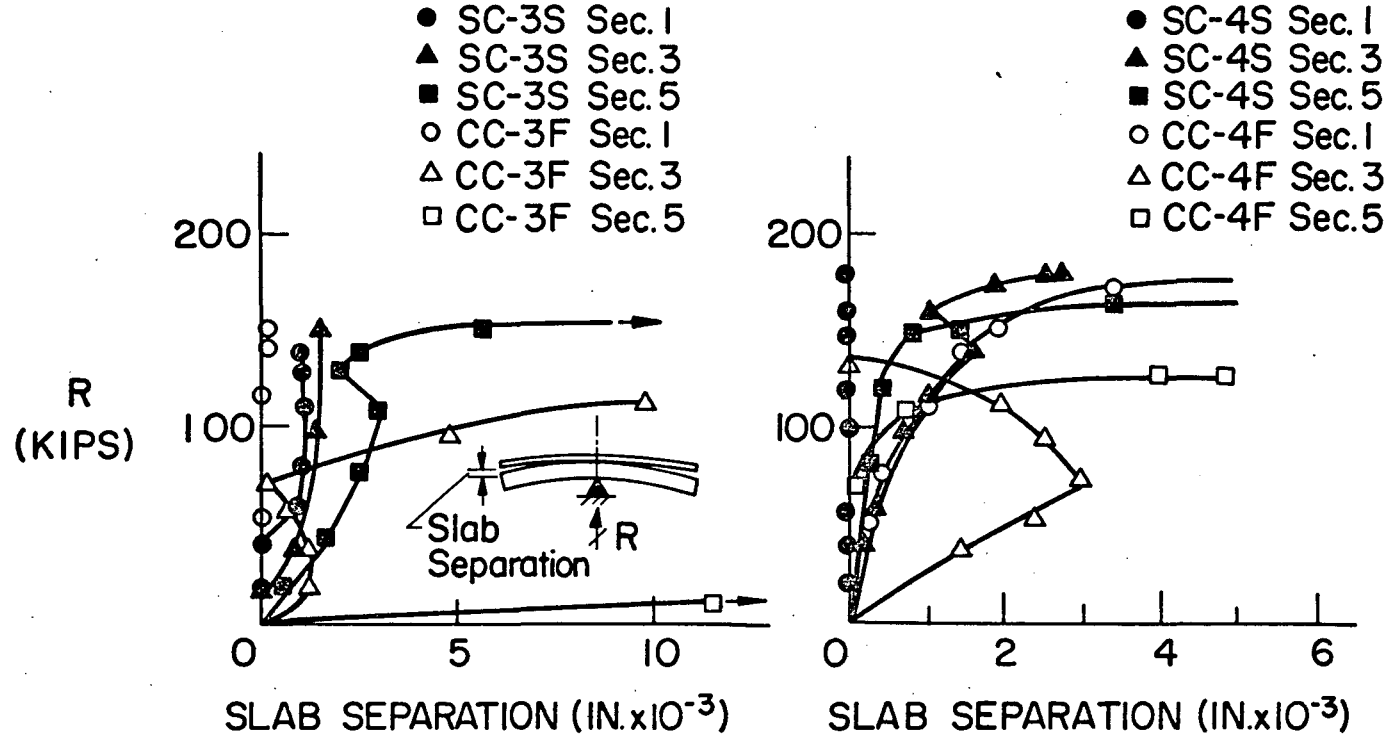

(b) Slab Separation Behavior

FIG. 20 SLIP AND SLAB SEPARATION BEHAVIOR

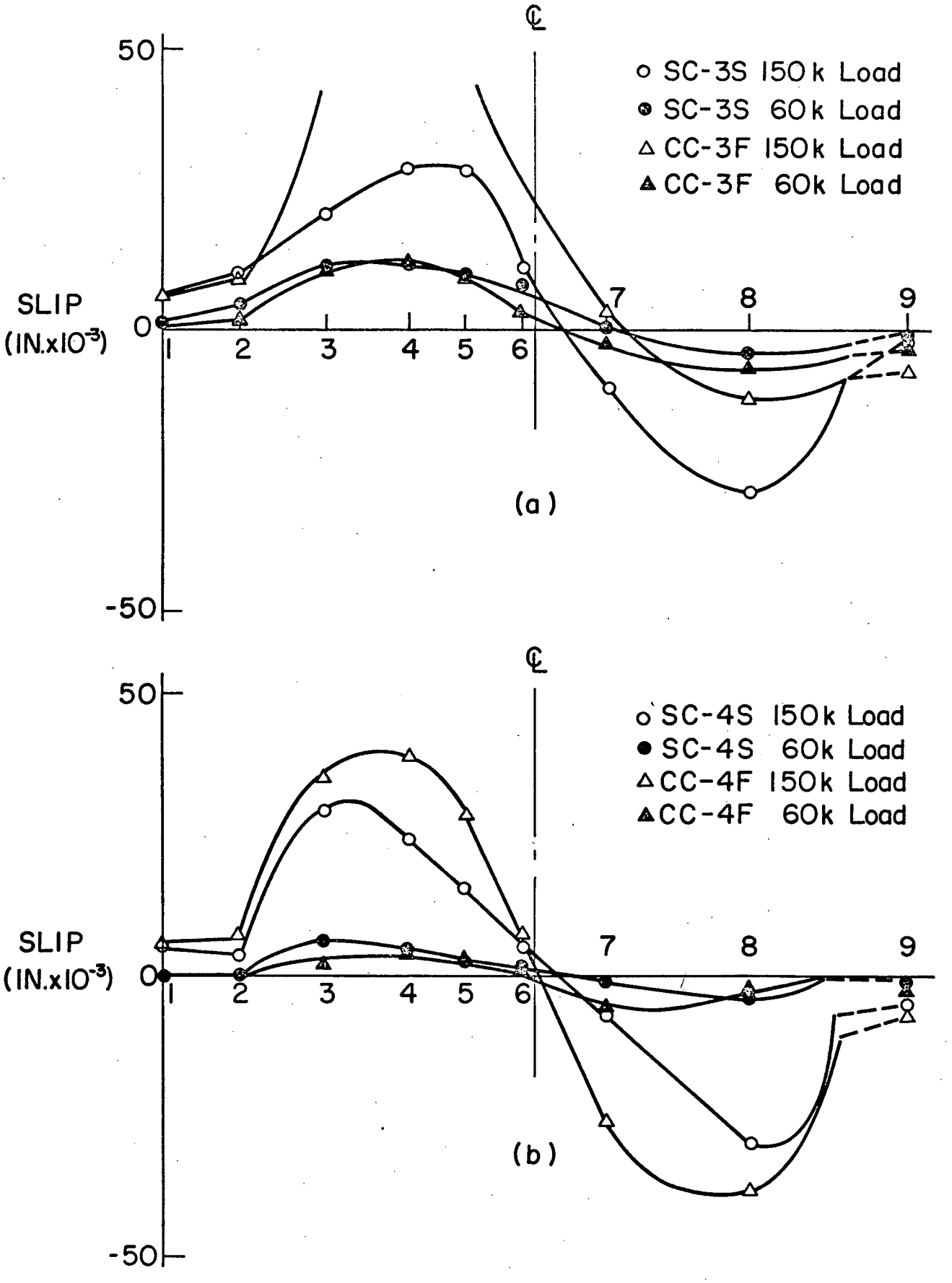

FIG. 21 SLIP DISTRIBUTION DIAGRAMS

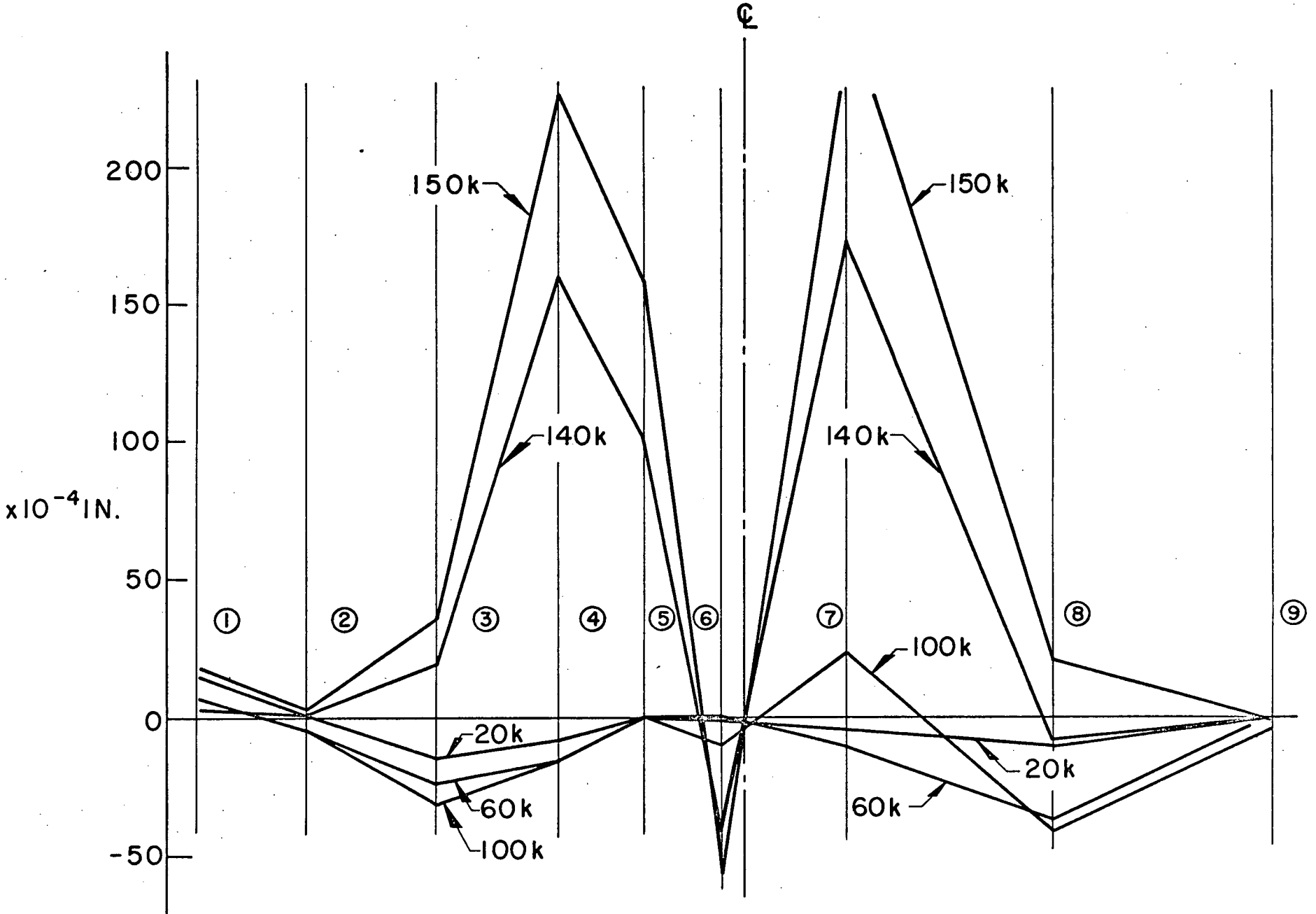

FIG. 22 DISTRIBUTION OF THE SEPARATION FOR BEAM CC-4F

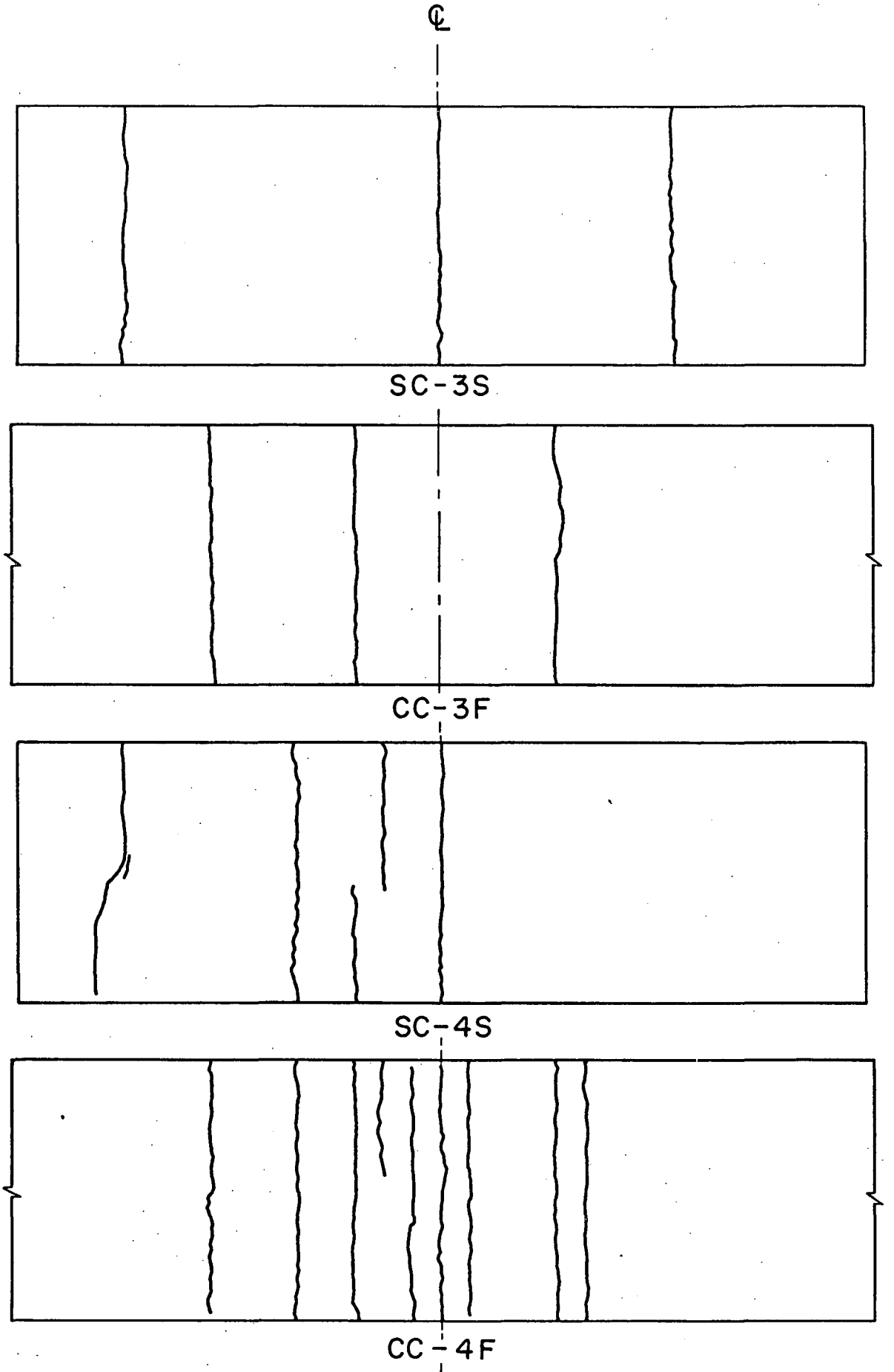

FIG. 23 CRACK PATTERNS AT WORKING LOAD LEVEL

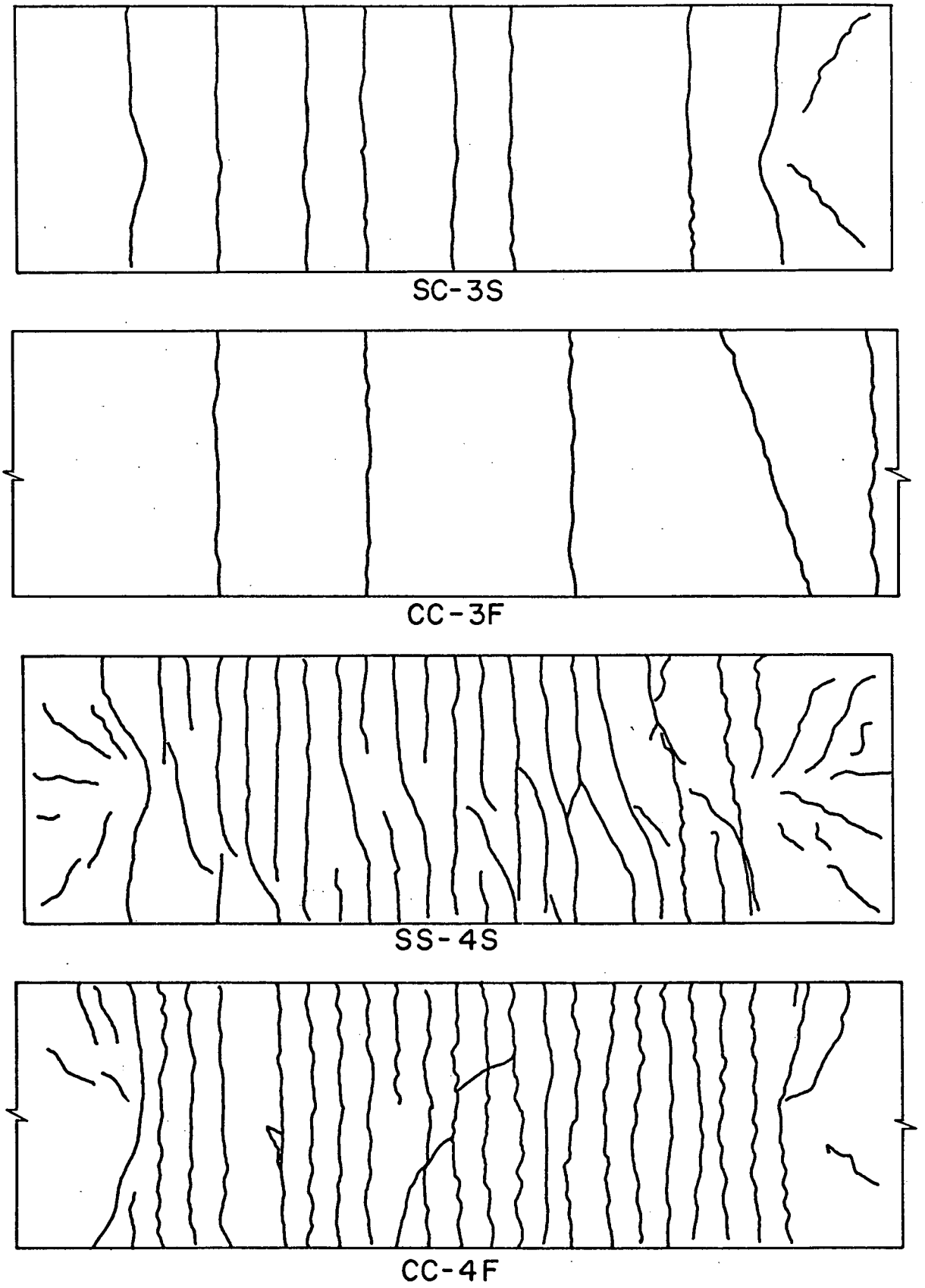

FIG. 24 CRACK PATTERNS NEAR ULTIMATE LOAD

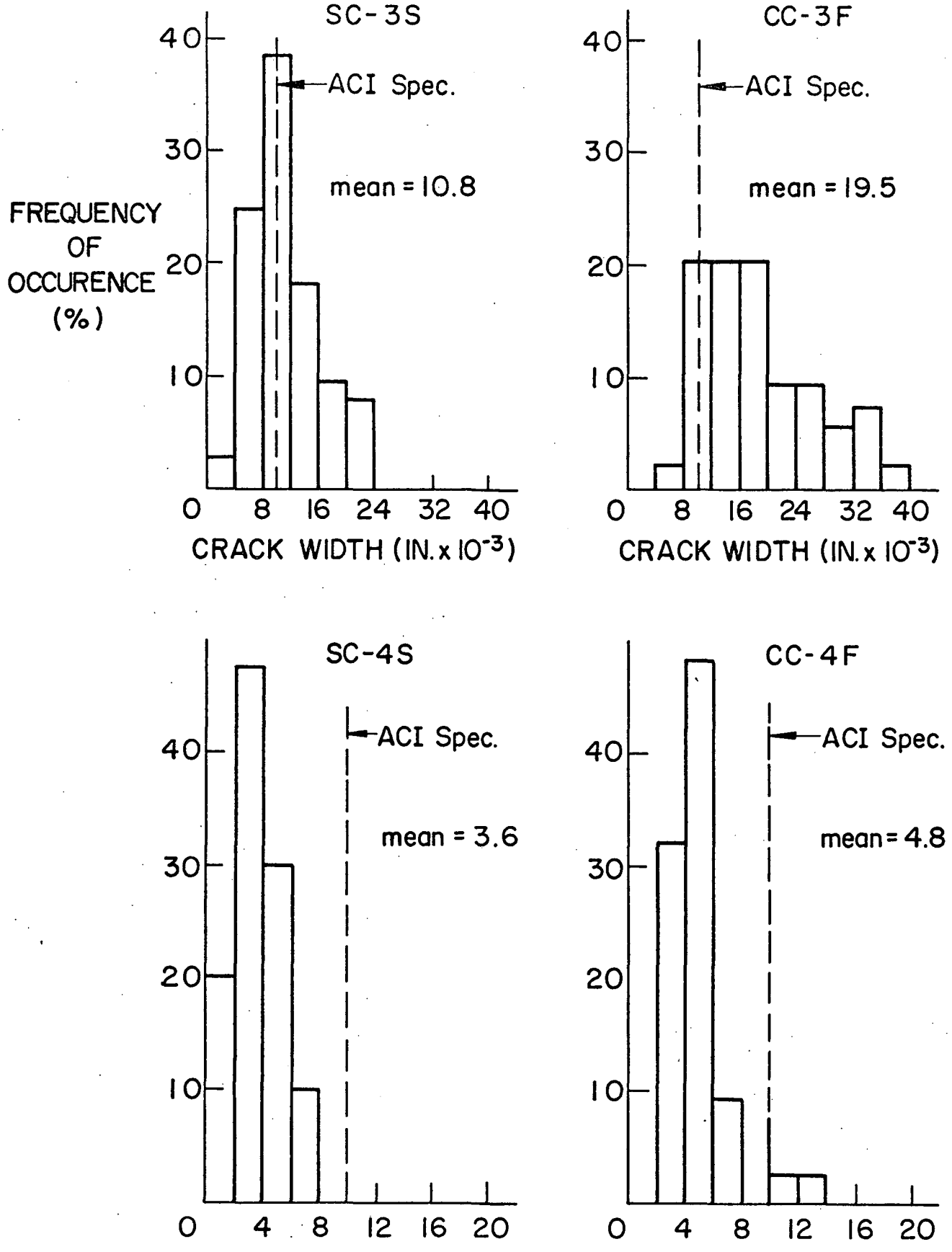

FIG. 25 CRACK WIDTH OCCURRENCE

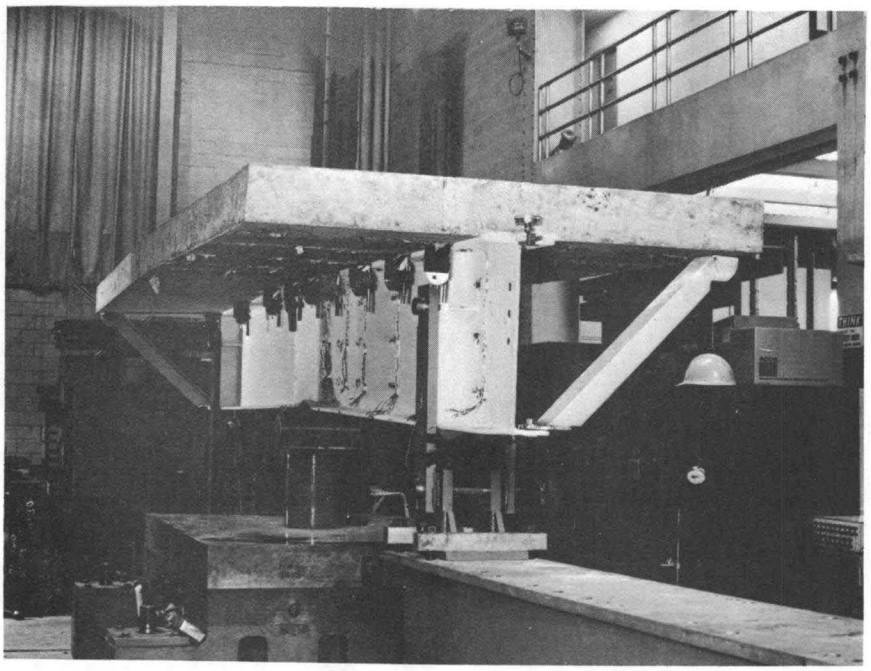

FIG. 26 BEAM AFTER FAILURE

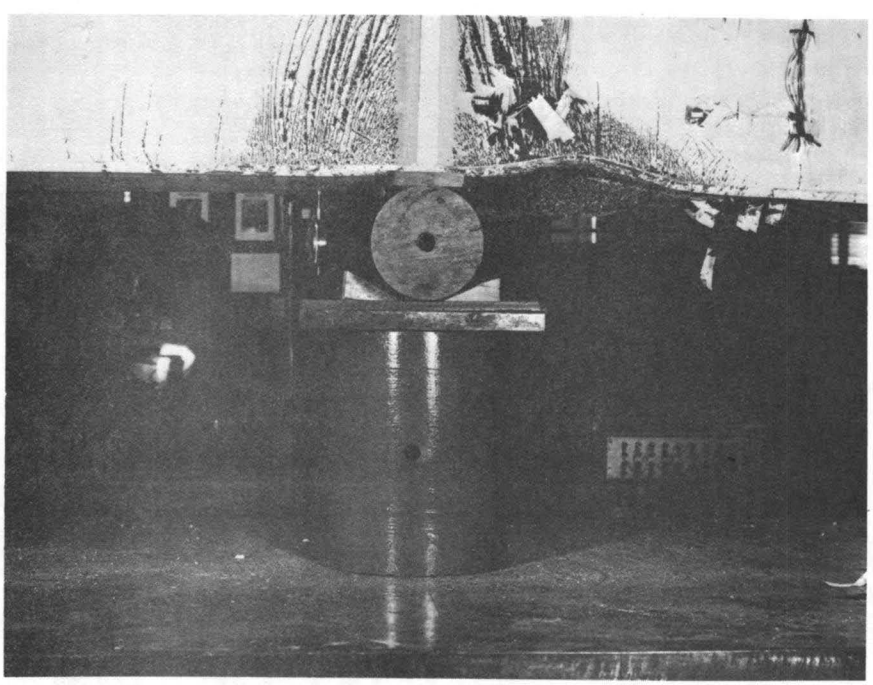

FIG. 27 LOCAL BUCKLING FAILURE MODE

7. REFERENCES

1. Daniels, J. H., and Fisher, J. W.
   FATIGUE BEHAVIOR OF CONTINUOUS COMPOSITE BEAMS, Highway Research Record No. 253, Highway Research Board, 1968, pp. 1-20

2. STANDARD SPECIFICATIONS FOR HIGHWAY BRIDGES, Tenth Edition by American Association of State Highway Officials, 1969

3. Slutter, R. G. and Fisher, J. W.
   FATIGUE STRENGTH OF SHEAR CONNECTORS, Highway Research Record No. 147, Highway Research Board, 1966, pp. 65-88

4. Wu, Y. C., Slutter, R. G. and Fisher, J. W.
   CONTINUOUS COMPOSITE BEAMS UNDER FATIGUE LOADING, Fritz Engineering Laboratory Report No. 359.2, Lehigh University, September 1970

5. Tall, L. et al
   STRUCTURAL STEEL DESIGN, Ronald Press Co., New York, New York, 1964

6. Park, R.
   THE ULTIMATE STRENGTH OF CONTINUOUS COMPOSITE T-BEAMS, Concrete Symposium, 1967, Institution of Engineers, Australia

7. Garcia, I., and Daniels, J. H.
   VARIABLES AFFECTING THE NEGATIVE MOMENT BEHAVIOR OF COMPOSITE BEAMS, Fritz Engineering Laboratory Report No. 359.3, Lehigh University, (In Preparation)

8. Garcia, I., and Daniels, J. H.
   NEGATIVE MOMENT BEHAVIOR OF COMPOSITE BEAMS, Ph.D. Dissertation, Fritz Engineering Laboratory Report No. 359.4, Lehigh University, January 1971